APPLICATION OF DE-EMBEDDING METHODS TO MICROWAVE CIRCUITS

by

Adam Swiatko

Submitted in partial fulfilment of the requirements for the degree

Master of Engineering (Electronic Engineering)

in the

Department of Electrical, Electronic and Computer Engineering

Faculty of Engineering, Built Environment and Information Technology

UNIVERSITY OF PRETORIA

January 2013

SUMMARY

APPLICATION OF DE-EMBEDDING METHODS TO MICROWAVE CIRCUITS

by

Adam Swiatko

Supervisor: Prof J.A.G. Malherbe

Department: Electrical, Electronic and Computer Engineering

University: University of Pretoria

Degree: Master of Engineering (Electronic Engineering)

Keywords: Calibration, Characterisation, Error Network, De-embedding, Offset Short, Unterminating,

In many instances the properties of a network are obstructed by an intervening network, which is required when performing measurements of the network. These intervening networks are often in the form of a mode transformer and are, in the general sense, referred to as error networks.

A new analysis mechanism is developed by applying a de-embedding method that was identified as being robust. The analysis was subsequently implemented in a numerical computational software package. The analysis mechanism can then be applied to perform the characterisation of error networks. The performance of the analysis mechanism is verified using an ideal lumped-element network. The limitations of the mechanism are identified and possible ways of addressing these limitations are given. The mechanism is successfully applied to the characterisation of three different microwave networks.

OPSOMMING

TOEPASSINGS VAN ONTBEDDENDE METODES OP MIKROGOLF STROOMBANE

deur

Adam Swiatko

Studieleier: Prof J.A.G. Malherbe

Departement: Elektriese, Elektroniese en Rekenaaringenieurswese

Universiteit: Universiteit van Pretoria

Graad: Magister in Ingenieurswese (Elektroniese Ingenieurswese)

Sleutelwoorde: Kalibrasie, Karakterisering, Fout Netwerk, Ontbeddende, Verskuifte Kortsluiting, Ontbeëindiging,

In baie gevalle word die eienskappe van die netwerk belemmer deur ‘n netwerk wat tussen-in geplaas word en wat benodig word vir meetings. Hierdie tussen-netwerke is dikwels in die vorm van ‘n modustransformator en word in die algemeen na verwys as foutnetwerke.

‘n Nuwe analisemetode is ontwikkel deur die toepassing van ‘n ontbeddende metode wat as robuust geïdentifiseer is. Die analise was daaropvolgend geïmplementeer in ‘n numeriese berekeningsprogrammatuur-pakket. Die analisemetode kan dan toegepas word om die karakteriseering van foutnetwerke uit te voer. Die werkverrigting van die analise meganisme is bevestig deur die gebruik van ‘n ideale punt-element netwerk. Die beperkings van die meganisme word geïdentifiseer en moontlike maniere om hierdie beperkings aan te spreek word gegee. Die meganisme is suksesvol toegepas op drie verskillende mikrogolf netwerke.

ACKNOWLEDGEMENT

The success of this work required a great deal of guidance and assistance from many different parties and I would like to take this opportunity to extend my sincerest gratitude to everyone involved.

A special thank you I extend to the Telkom Centre of Excellence and the CeTEIS group for the financial aid and for granting me access to a comfortable work environment with all the computing power and access to research materials that I needed to complete my research. Also, the exposure to the SATNAC conference was invaluable.

I owe my profound gratitude to my research supervisor Prof. J. A. G. Malherbe who dedicated his expertise, patience and time to this work and expressed a keen interest in seeing it through to the end. The regular meetings and discussions we had kept my spirits up and motivated me to keep at it. Thank you Prof.

Thank you to my friend Mr. T. R. Botha for his help with the development of the final application. Also a thank you to Mr. L. Naude, from the Compact Antenna Test Range, for his assistance and patience during the testing stages of the work.

My biggest thanks go towards my family, friends and especially Jess for all the support and encouragement they showed me during this period.

LIST OF ABBREVIATIONS

ANA	Automatic Network Analyser
CAD	Computer-Aided Design
CPW	Coplanar Waveguide
DUT	Device Under Test
EM	Electromagnetic
FDTD	Finite Difference Time Domain
FEM	Finite Element Method
GA	Genetic Algorithm
MoM	Method of Moments
SFD	Closed Loop Signal Flow Diagram
S-parameter	Scattering Parameter
TRL	Through, Reflect and Line
TSD	Through, Short and Delay

TABLE OF CONTENTS

CHAPTER 1

INTRODUCTION

1.1 BACKGROUND AND MOTIVATION

All electronic transmission networks have a need for some sort of mode transformer or matching circuit to be present between the source and the device under test (DUT), as is shown in figure 1.1. This is done to ensure that the maximum amount of power is delivered from the source to the device. The presence of the mode transformer has an effect on the network as it imparts its own transmission properties to the measurement of the device. As a result of this the measurements taken of the network do not explicitly express the characteristics of that device in isolation.

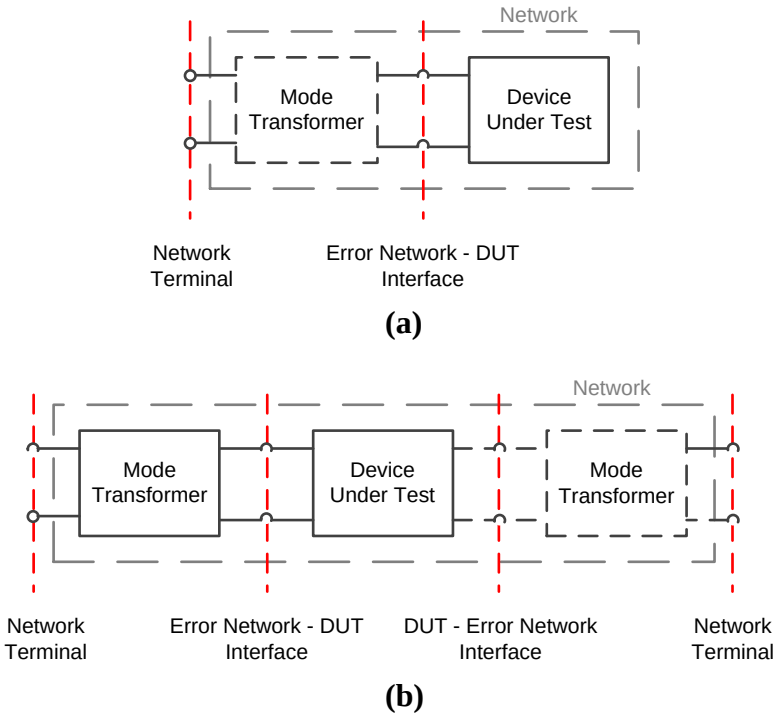

Figure 1.1. Block diagram of (a) a two section one-port network and (b) a three section two-port network comprising mode transformer(s) and a DUT.

The presence of a mode transformer in a network obscures the performance of the device it is driving. A method to isolate the transmission properties of the device from the transmission properties of the network is necessary. The application of de-embedding methods allows for a section of a network to be characterised indirectly [1], [2]. By applying de-embedding methods to the transmission properties of a network the transmission properties of the device can be isolated from the transmission properties of the mode transformer.

Given the advantages that software based prototyping can offer it can form the basis of a powerful means to develop new devices. Combining this with a method to remove the characteristics that the feeding section imposes on a device permits more control over the network as a whole. For this reason it is proposed that an application, using de-embedding methods and methodology, is developed to perform the desired network section isolation.

Certain properties have to be considered in the choice of de-embedding method to be used for such an application. The specifications for a desirable de-embedding method are,

(i) The method must not be complex. This will reduce the computational requirements needed to perform the de-embedding.

(ii) The method must be robust and capable of being applied to different types of microwave circuit structures. These include microstrip, waveguide, ridged waveguide, etc.

(iii) The method should be implemented in an application that is independent of the electromagnetic simulation package used to model the network.

1.2 RESEARCH OBJECTIVE AND QUESTIONS

1.2.1 Research Objectives

The focus of this study is to identify de-embedding methods that can be used to characterise and isolate the transmission properties of the mode transformer separate from the transmission properties of the network it might be connected to, and subsequently to implement the de-embedding method in a stand-alone application. The objectives of the study are,

(i) The primary objective was the identification of an adequate, or combination of adequate, de-embedding methods that are of a relatively low complexity and that can be applied to a variety of different microwave structures.

(ii) Secondly a selection of structurally different microwave circuits will be investigated and modelled in the appropriate simulation package and the transmission properties of these structures will be characterised using the de-embedding method.

(iii) Finally the de-embedding method will be implemented in a platform independent application.

1.2.2 Research Questions

The following are the research questions that will be addressed by this study.

(i) Can de-embedding methods be used to characterise the transmission properties of a microwave transition circuit.

(ii) Which de-embedding method, or combination of de-embedding methods, is most suited to develop a mechanism for analysis.

(iii) Can this tool be applied to characterising the transmission properties of a coaxial to double ridged waveguide mode transformer.

1.3 HYPOTHESIS AND APPROACH

1.3.1 Hypothesis

It is hypothesised that an analysis mechanism can be developed by implementing de-embedding methods. This can be done by using a combination of a numerical computational software package and a full-wave electromagnetic (EM) modelling and simulation software package. This tool can then be used to characterise the transmission properties of a chosen section of microwave circuit in isolation from the rest of the network.

1.3.2 Approach

The first step is to identify and verify the de-embedding method, or methods, that are most suited to the development of the desired analysis mechanism. The necessary mathematical manipulation software, required to extract the transmission properties of the desired section from the transmission properties of the system, would be developed in a numerical computational software package. Once this is found to perform satisfactorily, a model of the structure will be created in EM modelling and simulation software. The calculated simulation results would then be imported into the developed mathematical manipulation software to perform the de-embedding process and the final results will be compared to the a priori knowledge of the modelled network. The final step will be the application of the developed analysis mechanism to characterise the transmission properties of a given physical structure. Once it is shown that the analysis mechanism can be used to characterise the desired section of a microwave circuit it will be applied to the characterisation of a double ridged waveguide structure.

1.4 RESEARCH CONTRIBUTION

The evaluation and identification of de-embedding methods, which can be implemented in an analysis mechanism, and be applied to characterising the transmission properties of a given section of a network in isolation from the rest of the network. Currently no such platform independent analysis mechanism is readily available.

1.5 OVERVIEW OF STUDY

Chapter 1 provides an introductory background, the motivation, the objective as well as the contribution made by this work. The remainder of this dissertation is laid out below.

In Chapter 2 an introduction to de-embedding methods and methodology is presented and the electrical standards used in de-embedding methods are tabulated. Thereafter a large variety of de-embedding methods are examined and the de-embedding methods are organised into two distinct classes.

In Chapter 3 the efficacy of the de-embedding methods for purposes of arbitrary network characterisation is evaluated. The three offset short de-embedding method is identified as the most robust de-embedding method for the purposes of network characterisation. The method was implemented in MATLAB and was verified using a test network. Finally the MATLAB algorithm was implemented in a C++ based application.

In Chapters 4, 5 and 6 the three offset short de-embedding method is applied to the characterisation of three different networks. The three networks are a parallel line feed, a coaxial to rectangular waveguide mode transformer and a coaxial to double ridged waveguide mode transformer, respectively. The de-embedded results are compared to prior performance knowledge of the respective networks.

Chapter 7 is the conclusion of the work comprising a short summary of the work done as well as possible other applications of the work.

CHAPTER 2

DE-EMBEDDING METHODS

2.1 INTRODUCTION

De-embedding is the process of characterising the electrical properties of a device that is obscured by the electrical properties of a different device, a mode transformer, and can therefore not be characterised directly. Unterminating is the process of characterising the electrical properties of the mode transformer that is responsible for the obscuration [1]. Another term that carries a similar meaning as unterminating is calibration. This is a particular reference to the calibration of Automatic Network Analyser (ANA) connectors by means of known electrical standards, in order to remove its effects on the measured properties of a DUT. For the purpose of this work the three terms are treated as one and the same and are referred to as de-embedding.

A number of de-embedding methods have been reported [1] - [40] and with the advances in electronics producing smaller devices, many of the methods have been developed for, and tested on, on-wafer devices [19] - [29]. While the medium in which they are implemented is different, the methodology behind these de-embedding methods is generic and can be applied to other structures as well.

The reported de-embedding methods can be categorised into two distinct classes. One is an analytically based class where the networks are described by means of a cascade of matrices, a closed loop signal flow diagram representation of the network or an equivalent circuit model of the network [3] - [29]. The other class is a numerically based class where the networks are calculated by means of numerical techniques such as Finite-Difference Time-Domain (FDTD) [30], [31] or Method of Moments (MoM) [32] - [35]. In some recent cases Genetic Algorithms (GA) were implemented to perform the de-embedding [39], [40].

An aspect common to all the reported de-embedding methods is the definition of reference plane locations along the network. These are necessary as they define which section of the

network is to be treated as the DUT and which is to be treated as the rest of the error network in which the DUT is embedded. The location of the reference planes is in the general sense not important as long as it remains constant for the duration of the de-embedding process [3]. If the reference planes are defined so that it includes the ANA connector lines then a one-tier de-embedding procedure can be performed to isolate the DUT whereas if the reference plane is defined at the ends of the ANA connector lines then a two-tier de-embedding procedure needs to be performed where first the ANA is calibrated to remove the effects of the ANA and/or its connecting lines from the measurements and only then can the DUT be de-embedded [16].

Also common to all the de-embedding methods is the use of either known electrical standards to replace the DUT, or the use of equivalent circuit models used to describe the error networks surrounding the DUT.

A summary of the electrical standards used in de-embedding methods, along with a brief description of each, is given in table 2.1.

Table 2.1. Summary of electrical standards used for de-embedding.

Electrical Standard	Description
Short	A network termination with $\Gamma_L = -1$
Open	A network termination with $\Gamma_L = +1$
Reflect	Either a Short or an Open network termination
“Delay” or “Length” or “Line”	A length of network imparting a phase shift
“Through” or “Thru”	A network of zero length (direct connection)
Attenuator	A length of network with a high α
Match	A network termination with $\Gamma_L = 0$
Network	A network termination with $\{\Gamma_L \in \mathbb{C} \| \|\Gamma_L\| \leq 1\}$
Reciprocal	A network where the forward and reverse transmission coefficients are equal

The "Through" or "Thru" electrical standard is created by directly cascading two sections of a network, without the presence of an electrical standard section between them. This is equivalent to using a Line standard of zero length. If the two sections are identical then any phase shift measured for the network can be bisected thus characterising the phase shift introduced by the individual sections.

2.2 ANALYTICALLY BASED DE-EMBEDDING METHODS

The analytical class of de-embedding methods can be further broken down into three sub-groups which define how the network is represented.

2.2.1 Cascade Matrix Network Representation

The network is described as a cascade of matrices,

$$[T_{\text{Total}}] = [T_{\text{Error Network A}}][T_{\text{DUT}}][T_{\text{Error Network B}}]. \tag{2.1}$$

This is true if the network is a two- or multi-port network and the "error networks" are terminated at the network terminals in matched loads.

Each matrix represents a section of the network as is defined by the choice of reference plane location. The placement of the reference planes is arbitrary but in most cases the reference planes are placed at the terminals of the respective section. This placement of the reference plane in a network is represented graphically by figure 2.1, which also corresponds to equation (2.1).

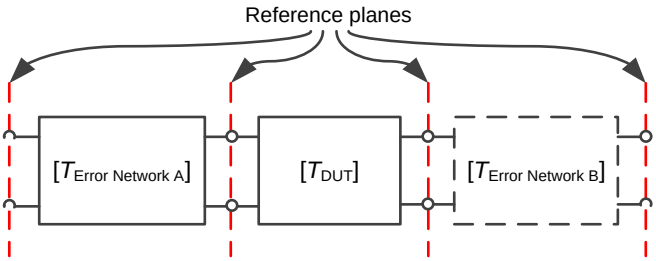

Figure 2.1. A cascade of matrices representation of a three section network showing the reference planes of the network.

For a two-port network each matrix would be of size 2x2 and each element of a matrix would correspond to the coefficients of that section, which would dependent on the form the matrix was in, for example the ABCD matrix form. The first step of the de-embedding methods is to characterise the properties of the error networks encapsulating the DUT. This is done by replacing the DUT with a variety of electrical standards and obtaining a measurement for each configuration. The properties of the error networks are then extracted from the measurements using closed form equations of the de-embedding methods. Once the error networks are characterised the DUT is replaced back into the network and a measurement of the network, which includes the DUT, is again performed. This measurement characterises the "Total" matrix of equation (2.1). The properties of the DUT are then extracted by means of straight forward matrix manipulation as expressed by

$$[T_{\text{DUT}}] = [T_{\text{Error Network A}}]^{-1}[T_{\text{Total}}][T_{\text{Error Network B}}]^{-1}. \tag{2.2}$$

One of the first reported de-embedding methods was a network calibration technique to remove the errors from the scattering parameter (S-parameter) measurements introduced by the connector lines of an ANA and it was performed using three unique electrical standards [3], the Through, the Short and the Delay (TSD). The network was modelled as a cascade of three 2x2 matrices where the outer matrices represent the "error networks" of the network and the central matrix represents the DUT, as per (2.1). The error networks are those sections of the network that obscure the properties of the DUT during measurements.

A non-iterative algorithm was developed to obtain the S-parameters of the two error networks. The authors were able to show that despite some hardware stability issues that contributed to measurement drift, the method showed great potential in a practical sense. This method was expanded into a more general form where the Short electrical standard was replaced by a Reflect electrical standard and this resulted in the formulation of the Thru-Reflect-Line (TRL) method [4]. This method became the backbone calibration method for ANA's [41]. It is still in use today and is considered the most accurate calibration method available in industry [42].

Even though the TRL method has been adopted by industry for the purposes of ANA calibration it should be noted that it does exhibit certain limitations as were reported in [5] and [6]. In [5] the TRL method exhibited frequency domain regions where it was considered to be not valid. This occurs when the Through standard is used and the measured phase shift of the network approaches half a wavelength in those frequency regions. In [6] the authors reported that using an arbitrary Reflection standard caused a phase uncertainty in the de-embedded results. This was due to the properties of the Reflection standard used being unknown. It was thus suggested that by using a Reflection standard of which the properties are precisely known, the phase uncertainty could, to a large extent, be removed. Alternatively, it was suggested that the Reflection standard be removed altogether from the de-embedding procedure. The resulting TL method makes use of only two electrical standards but thus requires that the network be assumed to be perfectly symmetrical for the de-embedding procedure to yield a unique solution. Further details about the number of electrical standards used for de-embedding and the respective accompanying assumptions that need to be made are given in Chapter 3.

A de-embedding method which evaluated the network section coefficients by using linear equations was reported in [7]. The de-embedding was then performed by simple matrix manipulation. This presented a generic approach to perform de-embedding. The approach was further expanded to describe special cases of the method where a variety of combinations of electrical standards were used. It also showed that the TRL and TSD

combinations fall under these special cases. The other special cases that were reported on are the Open-Short-Match (OSM), Through-Attenuator-Network (TAN), Through-Attenuator-Reflect (TAR), Through-Attenuator-Short (TAS), Through-Attenuator (TA), Through-Line (TL), Through-Match-Reflect (TMR), Through-Match-Short (TMS) and Through-Short-Open (TSO). Of these combinations the ones not using the Line standard avoided inherent bandwidth and low frequency limits that would present when the physical length of the transmission line was too long for practical use [7]. An extended version of the TMR method, the Line-Reflect-Match (LRM) method makes use of cascaded matrices to de-embed the S-parameters of the DUT [8]. A comparison of the LRM and Line-Reflect-Reflect-Match (LRRM) methods showed that the LRM method offers the same degree of accuracy but because one less electrical standard is required the de-embedding is performed faster.

Many of the de-embedding methods discussed to this point have made use of at least one Reflect electrical standard in the procedure. There are however cases of de-embedding methods where the Reflect standard is not needed [9] - [12]. In [9] and [10] the process requires only the use of two Line standards of different known lengths. The DUT, which is located in between the two error networks as per equation (2.1), is replaced by each of the Line standards. The network terminals of the two error networks are then attached to the connecting lines of an ANA, which have been pre-calibrated using a known calibration technique to be matched to the network characteristic impedance [42]. Thereafter a two-port measurement of the network is made for each Line standard. By assuming that the two error networks are identical and symmetrical allows the reciprocity principle to be applied, which reduces the number of coefficients that need to be characterised to two [43]. Once the error networks are characterised, the DUT is replaced back into the network and another two-port measurement is taken. Performing the de-embedding method yields a unique solution for the coefficients that describe the DUT. In [11] a similar approach is used as that in [9] and [10]. The difference in [11] is that only one Through standard is used instead of the two Line standards. This means that the two error networks are connected directly to each other in a back-to-back configuration. Here again it is assumed

that the two error networks are identical and symmetrical. Thereafter only one two-port measurement of the network is taken. The measured ABCD matrix, which describes that network, is bisected, thus characterising the two error networks of the network. Once the error networks have been characterised the de-embedding of the DUT is performed as previously discussed.

A unique de-embedding method, called the Line-Network-Network (LNN) method, is presented in [12]. In this de-embedding method the DUT is not replaced by electrical standards, as was previously discussed, instead the error networks are defined by unique electrical standards. “Error Network A” is defined as a reciprocal Network standard, described as an “obstacle” and of which the precise properties are unknown, placed at three different lengths along the transmission line between the defined network terminal and the device terminal. This forms the three unique electrical standards of this de-embedding method. “Error Network B” is defined as a Through and therefore does not impart anything on the measurements of the network. Three unique measurements of the network are taken, one for each of the three locations of the obstacle. A fourth measurement is also taken of just the transmission line with no obstacle present. Finally a closed form analytical algorithm is implemented to perform the de-embedding of the DUT. The method is expanded to a Double-LNN where the LNN method is performed on both sides of the DUT. This means that both error networks are replaced by the unique electrical standards of this method and which results in a total of six measurements that need to be made. The one advantage that this de-embedding method offers is as a result of the fixed positioning of the DUT that is being characterised. By not removing it from its fixture the possibility of measurement errors as a result of misalignments is greatly reduced.

2.2.2 Signal Flow Diagram Network Representation

The analytical class of de-embedding methods can be expressed as a closed loop signal flow diagram (SFD). A three section network, described by its S-parameter signal flow diagram, is shown in figure 2.2.

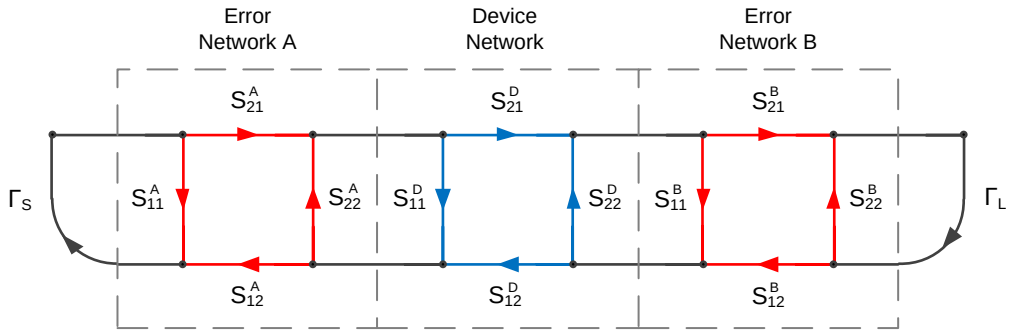

Figure 2.2. Signal flow diagram of a three section network, including the generator and load paths.

This form of network representation is preferred when working with a network that is described by its S-parameters.

In [13] a de-embedding method was described where a two-port error network is characterised by terminating the error network in three offset short standards. The offsets are themselves two-port networks and are attached between the error network terminal and a terminating Short standard. With each offset being of a different length, three one-port networks are subsequently created [13]. The reflection coefficient for each offset short terminated network is measured and the length of the offset is noted. The analytical equations for the de-embedding method are derived from the SFD of the network along with the circuit theory described in [44] and [45]. This generates three unique equations for the three error network unknowns that require characterising. The de-embedding method is then implemented to investigate what effect the use of an incorrectly defined offset length has on the performance of the de-embedding method.

The work done in [13] was then expanded and a full set of equations for this de-embedding method are derived in [14]. A de-embedding method based on the one described in [14], but where the Short standard is replaced by a Network standard of which the properties are known, is reported in [15]. The fundamental approach of these two methods is identical but the use of the Network standard makes it possible to make two-port measurements of the network. Doing this removes the need to assume that the network is reciprocal but rather

the forward and reverse transmission coefficients can be compared and reciprocity can be verified.

The method described in [16] makes use of three electrical standards, the Short, the Open and the Through. It then describes the network using the matrix description approach to generate a 4x4 error matrix. The error parameters described by this matrix are the two connecting lines between the ANA connectors and the DUT mounting fixture as well as the input and output error parameters of the DUT mounting fixture itself. The analytical equations were then derived using Mason's rule [44], [45]. No results were presented for this method but the method is inherently wide-band because the three standards used for the de-embedding procedure are fundamentally different at all frequencies.

The de-embedding method described in [17] applies a combination of the matrix manipulation technique and the Mason's rule derived equation in [14]. What is unique to this method is the requirement placed on the Reciprocal standard used. A full knowledge of the Reciprocal standard is not necessary; only its forward transmission coefficient phase shift need to be known. If the DUT is known to be reciprocal it can be used as a standard in its own network de-embedding procedure. The other standards used are the Open, Short and Load (which has been defined as a Network in this text) thus creating the Reciprocal-Open-Short-Load (ROSL) method. Its performance, for a Coplanar Waveguide (CPW), was compared to that of the LRM de-embedding method and the behaviour showed very good agreement.

A de-embedding method that also uses a combination of the matrix manipulation and the SFD representation is described [18]. The method makes use of only two Line standards of different length, that are placed between the two error networks in a back-to-back two-port configuration. The circuit is analysed using Mason's rule and the S-parameters of the network sections are calculated. Limitations are noted at a frequency of approximately 15 GHz which corresponds to the physical separation of the Line standard approaching half a wavelength. These limitations are similar to the observations reported in [5].

The use of the SFD de-embedding approach has also been applied to characterising sections of on-wafer devices [19], [20]. Despite the change in physical structure the de-embedding approach is precisely the same as previously described. In [19] a very similar approach is used to that reported in [18], with the exception that a third electrical standard, the Through, was introduced into the de-embedding method. The network was again placed in a back-to-back configuration and Mason's rule was applied to derive the analytical equations of the network. The equations were then solved and the forward and reverse transmission coefficients of the error networks were thus obtained. The calculated and measured results were given and a good agreement was observed between them.

Presented in [20] is a method based on Mason's rule to perform a one-port de-embedding. The method was proposed as an alternative to the lumped element method (described in more detail later in this chapter), which experiences an inherent degradation in the capacitance value as the frequency increases beyond 30 GHz. This runaway capacitance may cause inaccurate network characterisation. By describing the network in terms of the S-parameters the inherent limitations of lumped elements are removed, allowing more reliable de-embedding results to be obtained at high frequencies. The proposed method uses only two electrical standards, the Short and the Open, but with that also enforces two conditions, the first being reciprocity and the second being symmetry of the network thus requiring only two S-parameters to be characterised. The DUT was a reverse biased Schottky diode and its de-embedded capacitance performance, for the new method, was shown to be constant up to 110 GHz as compared to the de-embedded capacitance performance of the lumped element method which diverged from the constant for frequencies greater than 30 GHz.

2.2.3 Lumped Element Equivalent Circuit Network Representation

A third form of representation of the analytical method based de-embedding methods is to model some of the sections of the network as a lumped element equivalent circuit described by its series and shunt impedances. This method is preferred for simple structures, such as a connector probe pad of an on-wafer device as the circuit complexity

for such a section is relatively low. An example of a connector probe pad lumped element equivalent circuit model, showing both a series and shunt impedance, is shown in figure 2.3.

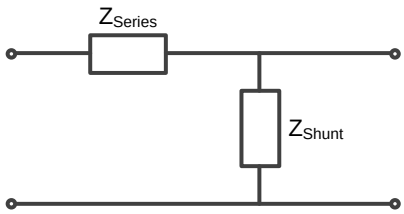

Figure 2.3. Equivalent circuit model of a connector probe pad or length of transmission line.

The various sections of the network are described by either their respective impedance or admittance matrix which can then easily be transformed to the corresponding S-parameter form.

De-embedding methods using the lumped element equivalent circuit have been reported several times in the past decade [21] - [29]. One of the earlier reports was [21] where the Open-Short (OS) de-embedding method is performed using an equivalent circuit model. Analytical equations are formulated from circuit theory and the unknown parameters can be calculated. Despite using a simple circuit model the performance of this method was in good agreement with a method that uses a comparatively more complex circuit model.

A de-embedding method using only two electrical standards was reported in [22]. The connecting lines were modelled as equivalent circuits and because the two electrical standards used for the method were the Open and the Through, a two-port de-embedding procedure could be performed. Once the transmission properties of the connecting lines were characterised, three different MOSFET's were substituted into the system as the DUT's. The results showed that the intrinsic noise parameters obtained from this de-embedding method were near identical to those calculated using the cascade matrix approach. The reported benefit of this method is the interconnect scalability that allows it

to be applied to DUT's of various physical sizes without having to re-evaluate the parasitic parameters of the interconnects each time.

As observed previously, not all the electrical standards are used in all the de-embedding methods. The use of only transmission electrical standards in on-wafer devices is commonly reported [23] - [29]. Often, only two Line standards, of different length, are used but in some cases a third Line standard is introduced of either no length, a Through, or of a third different length. From this point onwards the de-embedding procedure is the same as for the other equivalent circuit methods and the performance of the reported methods was found to be satisfactory in all the cases.

A limitation that has been observed with this approach to de-embedding is the simplicity of the circuit models used. This is acceptable when working with simple sections of networks, such as a transmission line, but becomes considerably more complex to work with as the network complexity increases. Also observed was a difference in results between using a T-network or a π-network equivalent circuit model. In [29] both equivalent circuit models were evaluated and the results compared to those obtained from a Through-Line (TL) de-embedding method. It was found that de-embedding using the T-network model yields results that are similar to those obtained for the TL de-embedding method, whereas the π-network model results compared less favourably.

2.3 NUMERICALLY BASED DE-EMBEDDING METHODS

The distinction between the numerically based de-embedding methods, as compared to the analytically based de-embedding methods from the previous section, is that the latter can be used to derive closed form equations which describe the network, whereas the former have the network described by integro-differential equations. Solution of these integro-differential equations necessitates that the network geometry be meshed over which the current or voltage distributions are calculated. This requires the definition of suitable current or voltage excitation as the source.

2.3.1 Finite-Difference Time-Domain De-embedding

In an FDTD analysis technique, for a two-dimensional microwave network, the network is segmented into equally sized blocks and the two-dimensional wave equation is solved for each segment [30]. The calculated voltages and currents are then transformed into S-parameters. The described method is applied to characterising a ring circuit, which had been previously characterised in a different publication, and the results presented very good agreement between the two methods. Also investigated were the effects the excitation pulses had on the calculations and it was found that the delta-type pulse was the most practical.

The circuit modelling technique using FDTD was extended to three-dimensional circuit analysis in [31]. This was developed to more accurately take into account the fringing, coupling and radiation effects of planar structures. The method was developed to calculate the S-parameters of the network being analysed by applying Fourier transforms. It is then applied to characterising a rectangular patch antenna, a microstrip lowpass filter, as well as a four-port branch line coupler. In all three cases the calculated and measured results showed very good agreement.

2.3.2 Method of Moment De-embedding

In [32] two different excitation models are investigated and compared against each other. The two excitation models are the delta-gap voltage and the induced-currents model. In order to compare these two models against each other their equivalence is first determined. The integral equations are then derived and an impedance matrix for a M-port network is developed. The excitation model relates to the impedance matrix through

$$[Z^t][I^t]=[V^t]. \tag{2.3}$$

Irrespective of which excitation model is used this method requires only one unknown parameter matrix to be determined. The network was then meshed and the impedance

matrix was determined. Once the impedance matrix was known it was transformed into the equivalent S-parameter matrix thus describing the network in terms of its transmission and reflection properties. The two methods were applied to characterising a single stub microstrip filter. The two sets of calculated results were in very good agreement when compared to the measured results for the single stub microstrip filter.

The de-embedding circuit characterisation method described in [33] uses a very similar approach to that described in [32], also using a delta-gap excitation model. The method is developed with the use of an arbitrary four-port network and then tested using a coupled-line bandpass filter which showed good agreement to measured results. The developed MoM de-embedding method is then applied to characterise a four-port branch line coupler, similar to the one described in [31], which was performed using the FDTD method. The results of the two methods showed good agreement.

De-embedding by means of MoM is applied in conjunction with the Short-Open Calibration (SOC) de-embedding method in [34]. The two electrical standards used, the Short and the Open, are modelled by use of an Electric wall and a Magnetic wall, respectively. The MoM based SOC method is used to characterise the connecting lines between the excitation port and the DUT, in terms of their voltages and currents, which are then explicitly described by their network matrices. The effects of microstrip end-to-end coupling are investigated using the developed MoM based SOC de-embedding method. The work on the MoM based SOC de-embedding method is then further developed to characterise the properties of nonuniform connecting lines [35].

2.3.3 Finite Element Method De-embedding

The FEM contains certain attributes that make it desirable for the purposes of de-embedding. The FEM is based on the boundary value problem, which is limited by boundary conditions, and is applied as an integral formulation which can be approximated by a polynomial. This is achieved by breaking the structure down into either surface or volume elements and solving the polynomial approximation for each element. The

advantage this offers is the ability to be applied to structures with irregular shapes as the elements can be made to fit the contours of the structure more precisely [36]. The versatility of the FEM based network characterisation technique has seen it being implemented in full-wave electromagnetic simulation packages such as CST Studio Suite [37].

The FEM can be used for the purposes of two-port network characterisation but implementing it as a SOC de-embedding method. The definition of the Short and Open electrical standards is similar to that found in [35], with the Short electrical standard being modelled as an Electric wall and the Open electrical standard being modelled as a Magnetic wall. The de-embedding method is applied to characterising several structures namely a coplanar waveguide to microstrip transition, an open ended microstrip structure, a microstrip coupling structure and a symmetric microstrip resonator structure. In all four cases the results were compared to respective published results and showed very good agreement [38].

Despite the robust nature of the FEM based de-embedding method for the purpose of network characterisation care needs to be taken when using it. The polynomial approximations of the integral functions may result in non-real solutions [36]. Also the FEM cannot be directly applied to characterising unbounded or infinite structures [38].

2.3.4 Genetic Algorithm De-embedding

De-embedding can also be performed by viewing the network characterisation as an optimisation problem and thus making use of a GA to determine the unknown parameters. In [39] de-embedding is performed by implementing a GA to obtain the transmission properties of a Through network. The method requires that both the upper and the lower limits of the unknown parameters be defined by the user as constraints for the GA. The method was verified by a comparison of measured and experimental results and it showed very good performance.

A de-embedding method which applies the GA to determine the unknown parameter at the first frequency, and thereafter a gradient fitting technique to determine the parameter value at the next frequency, based on the value of the previous point, was used in [40]. This method was applied to characterising a coaxial to waveguide transition using several one- and two-port electrical standards. The results of the proposed method were compared to measured results and showed very good agreement.

CHAPTER 3

DE-EMBEDDING BY MEANS OF THREE OFFSET SHORT ELECTRICAL STANDARDS

In this work the application of de-embedding methods to perform the error network characterisation was investigated. This means the DUT of the network shown in figure 2.1 was replaced by electrical standards of known properties, while simultaneously the error network became the focus of the network characterisation.

The de-embedding methods discussed in Chapter 2 have all been shown to perform satisfactorily for the networks that they were applied to. However, certain methods possess attributes that make them unattractive for de-embedding networks of a high structural complexity. These methods predominantly fall under the numerical class of de-embedding methods which in the case of FDTD, MoM and FEM require precise structural information of the network to be known. Thereafter a meshing of the structure must be performed to satisfy the integro-differential boundary conditions. In the publications reported thus far these three methods were applied to microstrip structures which, in many cases, were approximated as two-dimensional structures to simplify the mathematics. In some cases the work was expanded to a three-dimensional structure but this requires a three-dimensional meshing of the structure to be defined which will subsequently require a longer computational time to solve the integro-differential equations. These methods are better suited to network characterisation where the physical structure is defined in a computer-aided design (CAD) environment.

In the case of GA based de-embedding methods a broad a-priori knowledge of the transmission properties of the network are preferred to be used as GA constraints. This may not always be possible for an arbitrary error network. Also desired, for accurate network characterisation, is the definition of a very low error evaluation number to be used in the evaluation function stage of the algorithm. However, the choice of a small error evaluation number may cause the algorithm to perform a large number of iterations to meet the defined error requirement. The definition of a wide constraints range together with a

low error evaluation number may result in the de-embedding process to take a long time to complete. The GA based de-embedding methods are thus better suited as optimisation methods where the constraints range is relatively narrow.

Consequently, an analytically based approach to de-embedding was further investigated. The analytically based de-embedding methods were further narrowed down to comprise only the cascade matrix and signal flow diagram methods. This was due to the equivalent circuit methods requiring a detailed circuit model of the error network to be defined in order to avoid an over-simplification of the error network, which could lead to inaccuracies in the calculated properties. The equivalent circuit de-embedding methods are better suited to describing fairly simple networks such as the transmission line or connecting probe networks of a microstrip or on wafer structure. Therefore both the cascade matrix method and the signal flow diagram method were investigated for a suitable de-embedding method.

3.1 CASCADE MATRIX CONFIGURATION

Cascade matrices present a very convenient way of describing a network. Each section of the network can be represented by its own matrix; these matrices can be of the form ABCD, T, S or Z. Each of these matrix forms possesses unique attributes that give them preferred application.

The T-matrix is a transmission matrix form that can be cascaded and is thus ideally suited to the cascade matrix approach. In the case of network with balanced ports, i.e. a network that has the same number of input and output ports, a direct relationship exists between the T-matrix and the S-matrix form [46]. The direct conversion between T-matrix and S-matrix for a two-port network is given in table 3.1.

Table 3.1. T-matrix and S-matrix conversion table for a two-port network.

	S	T
S	$\begin{bmatrix} S_{11} & S_{12} \\ S_{21} & S_{22} \end{bmatrix}$	$\begin{bmatrix} \frac{T_{12}}{T_{22}} & T_{11} - \frac{T_{12}T_{21}}{T_{22}} \\ \frac{1}{T_{22}} & -\frac{T_{21}}{T_{22}} \end{bmatrix}$
T	$\begin{bmatrix} S_{12} - \frac{S_{11}S_{22}}{S_{21}} & \frac{S_{11}}{S_{21}} \\ -\frac{S_{22}}{S_{21}} & \frac{1}{S_{21}} \end{bmatrix}$	$\begin{bmatrix} T_{11} & T_{12} \\ T_{21} & T_{22} \end{bmatrix}$

The mathematical representation of a three sectioned network terminated at both network terminals in a matched network is given by (2.1), repeated in (3.1) for convenience.

$$[T_{\text{Total}}] = [T_{\text{Error Network A}}][T_{\text{DUT}}][T_{\text{Error Network B}}] \tag{3.1}$$

In this form the DUT is located inside the embedding network, which, in this case, is made up of the two error networks. These error networks can be as simple as a length of transmission line or more complex comprising many components. The de-embedding procedure, to characterise the DUT, requires that the Total matrix as well as the two error network matrices be determined first.

The Total matrix is obtained by terminating the network at both network terminals in a matched load and then by performing either a measurement on an ANA or by calculation of a model of the network in a full-wave EM simulation package.

The properties of the error networks can be characterised by replacing the DUT with electrical standards of which the properties are known. A measurement of the network containing each of the electrical standards, required for the de-embedding method, is made. Thereafter, the influence of the electrical standards are extracted by applying the cascade

matrix de-embedding methods reported in [3] - [12]. By applying matrix manipulations, such as those expressed in

$$\begin{aligned}[T_{\text{DUT}}] &= [T_{\text{Error Network A}}]^{-1}[T_{\text{Total}}][T_{\text{Error Network B}}]^{-1} \\ &= [T_{\text{Error Network A}}]^{-1}[T_{\text{Error Network A}}][T_{\text{DUT}}][T_{\text{Error Network B}}][T_{\text{Error Network B}}]^{-1}\end{aligned}, \tag{3.2}$$

the properties of the DUT can be then extracted.

The de-embedding method used to perform the error network characterisation is often governed by the availability of electrical standards. The replacement of the DUT by a known electrical standard is done because the performance of the electrical standard can be predicted and thus its influence on the measurement can be removed, subsequently extracting the network surrounding the electrical standard.

The choice of electrical standard dictates the configuration of the measurement that can be made. The use of the Line, Through or Network standards allows for a two-port measurement of the network to be taken. This is expressed by both the reflection and transmission coefficients of the network. Making the assumption that the two error networks are identical allows the network to be placed in a back-to-back configuration.

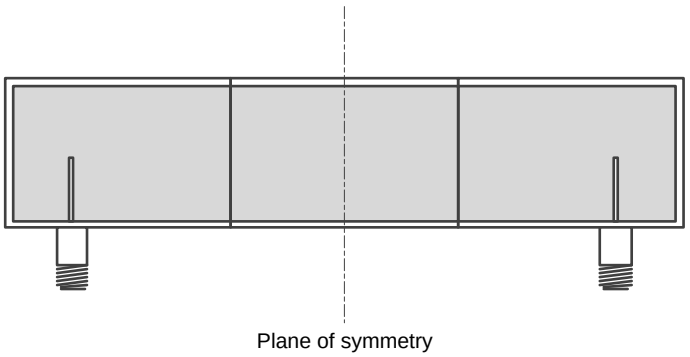

Figure 3.1. Cross-sectional view of a two-port waveguide network in a back-to-back configuration.

Figure 3.1 shows a cross-sectional back-to-back configuration of two coaxial to rectangular waveguide mode transformers with an arbitrary length of waveguide between them.

There are eight error network unknowns that need to be characterised in a two-port back-to-back network. Since the electrical standards used are passive devices, the principle of reciprocity may be applied. This reduces the number of unknowns that need to be determined to six as expressed by

$$\begin{aligned}\begin{bmatrix} T_{11_{\text{Total}}} & T_{12_{\text{Total}}} \\ T_{21_{\text{Total}}} & T_{22_{\text{Total}}} \end{bmatrix} &= \begin{bmatrix} T_{11_{\text{A}}} & T_{12_{\text{A}}} \\ T_{21_{\text{A}}} & T_{22_{\text{A}}} \end{bmatrix} \begin{bmatrix} T_{11_{\text{Line}}} & T_{12_{\text{Line}}} \\ T_{21_{\text{Line}}} & T_{22_{\text{A}}} \end{bmatrix} \begin{bmatrix} T_{22_{\text{B}}} & T_{21_{\text{B}}} \\ T_{12_{\text{B}}} & T_{11_{\text{B}}} \end{bmatrix} \\ &= \begin{bmatrix} T_{11_{\text{A}}} & T_{12_{\text{A}}} \\ T_{12_{\text{A}}} & T_{22_{\text{A}}} \end{bmatrix} \begin{bmatrix} 0 & T_{12_{\text{Line}}} \\ T_{12_{\text{Line}}} & 0 \end{bmatrix} \begin{bmatrix} T_{22_{\text{B}}} & T_{12_{\text{B}}} \\ T_{12_{\text{B}}} & T_{11_{\text{B}}} \end{bmatrix} \\ &= \begin{bmatrix} T_{12_{\text{Line}}}\left(T_{12_{\text{A}}}T_{22_{\text{B}}} + T_{11_{\text{A}}}T_{12_{\text{B}}}\right) & T_{12_{\text{Line}}}\left(T_{12_{\text{A}}}T_{12_{\text{B}}} + T_{11_{\text{A}}}T_{11_{\text{B}}}\right) \\ T_{12_{\text{Line}}}\left(T_{22_{\text{A}}}T_{22_{\text{B}}} + T_{12_{\text{A}}}T_{12_{\text{B}}}\right) & T_{12_{\text{Line}}}\left(T_{22_{\text{A}}}T_{12_{\text{B}}} + T_{12_{\text{A}}}T_{11_{\text{B}}}\right) \end{bmatrix}\end{aligned} . \quad (3.3)$$

This is done by making the forward and reverse transmission coefficients of each section equal.

If the two error networks are assumed to be identical the number of error network unknowns is reduced to three as is expressed by

$$\begin{bmatrix} T_{11_{\text{Total}}} & T_{12_{\text{Total}}} \\ T_{21_{\text{Total}}} & T_{22_{\text{Total}}} \end{bmatrix} = \begin{bmatrix} T_{12}T_{12_{\text{Line}}}\left(T_{22} + T_{11}\right) & T_{12_{\text{Line}}}\left(T_{12}^{\,2} + T_{11}^{\,2}\right) \\ T_{12_{\text{Line}}}\left(T_{22}^{\,2} + T_{12}^{\,2}\right) & T_{12}T_{12_{\text{Line}}}\left(T_{22} + T_{11}\right) \end{bmatrix} . \quad (3.4)$$

Furthermore, if the two error networks are assumed to be identical then the network becomes symmetrical around the plane symmetry shown in figure 3.1. This allows for the forward reflection coefficient at the two ports of the ANA to be assumed equal thus further reducing the number of unknowns that need to be determined to two as expressed by

$$\begin{bmatrix} T_{11_{\text{Total}}} & T_{12_{\text{Total}}} \\ T_{21_{\text{Total}}} & T_{22_{\text{Total}}} \end{bmatrix} = \begin{bmatrix} T_{12}T_{12_{\text{Line}}}\left(2T_{11}\right) & T_{12_{\text{Line}}}\left(T_{12}^{\ 2}+T_{11}^{\ 2}\right) \\ T_{12_{\text{Line}}}\left(T_{11}^{\ 2}+T_{12}^{\ 2}\right) & T_{12}T_{12_{\text{Line}}}\left(2T_{11}\right) \end{bmatrix}. \tag{3.5}$$

Now only two unique two-port measurements need to be made, each with a different two-port electrical standard.

In the case where the Through electrical standard is used the cascade matrices can be expressed as

$$\begin{aligned} \begin{bmatrix} T_{11_{\text{Total}}} & T_{12_{\text{Total}}} \\ T_{21_{\text{Total}}} & T_{22_{\text{Total}}} \end{bmatrix} &= \begin{bmatrix} T_{11} & T_{12} \\ T_{21} & T_{22} \end{bmatrix}\begin{bmatrix} T_{22} & T_{21} \\ T_{12} & T_{11} \end{bmatrix} \\ &= \begin{bmatrix} T_{11} & T_{12} \\ T_{12} & T_{11} \end{bmatrix}\begin{bmatrix} T_{11} & T_{12} \\ T_{12} & T_{11} \end{bmatrix} \\ &= \begin{bmatrix} T_{11}^{\ 2}+T_{12}^{\ 2} & 2\left(T_{11}T_{12}\right) \\ 2\left(T_{11}T_{12}\right) & T_{11}^{\ 2}+T_{12}^{\ 2} \end{bmatrix} \end{aligned}. \tag{3.6}$$

The use of Reflect standards allows for a one-port measurement of the network to be taken, which would be expressed by only the reflection coefficient. This removes the need for a back-to-back configuration allowing the error network to be directly terminated by the Short or Open electrical standard as expressed by

$$\begin{aligned} \begin{bmatrix} T_{11_{\text{Total}}} & T_{12_{\text{Total}}} \\ T_{21_{\text{Total}}} & T_{22_{\text{Total}}} \end{bmatrix} &= \begin{bmatrix} T_{11} & T_{12} \\ T_{21} & T_{22} \end{bmatrix}\begin{bmatrix} T_{11_{\text{R}}} & T_{12_{\text{R}}} \\ T_{21_{\text{R}}} & T_{22_{\text{R}}} \end{bmatrix} \\ &= \begin{bmatrix} T_{11} & T_{12} \\ T_{21} & T_{22} \end{bmatrix}\begin{bmatrix} T_{11_{\text{R}}} & 0 \\ 0 & 0 \end{bmatrix} \\ &= \begin{bmatrix} T_{11}T_{11_{\text{R}}} & 0 \\ 0 & 0 \end{bmatrix} \end{aligned}. \tag{3.7}$$

In all the cascade matrix de-embedding cases the use of more electrical standards than there are unknowns adds redundancy which can be used to test the accuracy of the error network characterisation.

Once the measurements of the network containing the electrical standards are made, the error networks can be characterised by simultaneously solving the algebraic equations derived from the cascaded matrices.

The cascade matrix de-embedding method presents a predictable and simple approach to network characterisation. A limitation of this method is the need for two-port measurements to be made. The reason for this is that the equations derived for the one-port measurements can only contain one characterisation unknown, it being the reflection coefficient, and thus cannot be used to perform a full error network characterisation.

For two-port measurements to be possible an ANA with two-port capabilities needs to be available. Also required are two identical error networks to reduce the number of unknowns that need to be characterised, which subsequently reduces the number of unique electrical standards needed for the de-embedding method.

If the error network characterisation, of a back-to-back configured network, is to be performed in an EM simulation package the two-port model would be very large as it would have to comprise two error networks as well as the electrical standard. For complex three-dimensional structures this results in simulation files that are considerably larger than if only a single error network is characterised, which may cause the memory requirement of the simulation package to be exceeded.

These limitations do not fully comply with the robustness requirement defined in section 1.1 (ii), thus making this de-embedding method not desirable for error network characterisation.

3.2 SIGNAL FLOW DIAGRAM CONFIGURATION

The SFD representation is another convenient way of describing a network. As with the cascade matrix method discussed previously, the network can be divided into adjacent sections. Where the SFD method differs from the cascade matrix method is that each section is described by a unique SFD. A SFD is a graphical representation of a set of linear relations, comprising nodes, directional branches and loops [47]. The sections can be in the S-parameter form which relates the output and input voltages of each branch. The S-parameter form is desirable as most ANA's and EM simulation packages can output data in this form. An S-parameter SFD of a single section two-port network, including a source and load path, is shown in figure 3.2.

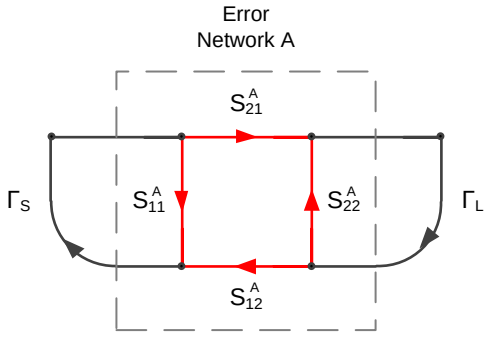

Figure 3.2. Signal flow diagram of a single section two-port network including source and load paths.

The transfer function of a network is derived by examining the forward and loop paths that are formed by the nodes and branches, paying attention to the combinations of non-touching loops. Non-touching loops are loop paths in a network that do not share a node. The algebraic transfer function to compliment the SFD can be derived from Mason's rule [44], which is expressed by

$$M = \frac{\sum_k M_k \Delta_k}{\Delta}, \tag{3.8}$$

where

M_k = path gain of the kth forward path

Δ = 1 – Σ (all individual loop gains)
+ Σ (loop gain products of all combinations of two non-touching loops)
– Σ (loop gain products of all combinations of three non-touching loops)
+ …

Δ_k = the value of Δ not touching the kth forward path.

A network comprising more sections can be described by cascading two or more of the single section SFDs. The ends of each section are defined by the reference planes, which are represented by a node at the source and load of the network. The reference planes are often chosen at the physical terminations of the structure the SFD is representing. A three section SFD is shown in figure 2.2 in Chapter 2.

In [45] equation (3.8) was applied to an S-parameter network, such as that shown in figure 3.2, to derive a closed form equation for a single sectioned two-port SFD network. The resulting S-parameter closed form equation for the network is given by

$$\rho = S_{11} + \frac{S_{21}S_{12}\Gamma_L}{1 - S_{22}\Gamma_L} \ . \tag{3.9}$$

This is a simplified equation where the source is assumed to be matched. Because the network only comprises one loop the resulting closed form equation is fairly simple.

Terminating the network in a Short or Open electrical standard the load reflection coefficient is replaced by ∓1, respectively, simplifying the equation to

$$\rho = S_{11} \mp \frac{S_{21}S_{12}}{1 \pm S_{22}} \ . \tag{3.10}$$

A network represented by an SFD can also be terminated in an arbitrary Network electrical standard as long as the input reflection coefficient of the terminating network is known.

However, terminating a single section SFD network in a matched load simplifies equation (3.9) to only yield the input reflection coefficient of the network. This does not carry enough information to be of any use for the purposes of network characterisation.

For a two sectioned SFD network, such as the one shown in figure 3.3, the network now presents more possible loop combinations making the resulting closed form equation, expressed by equation (3.11), considerably more complex.

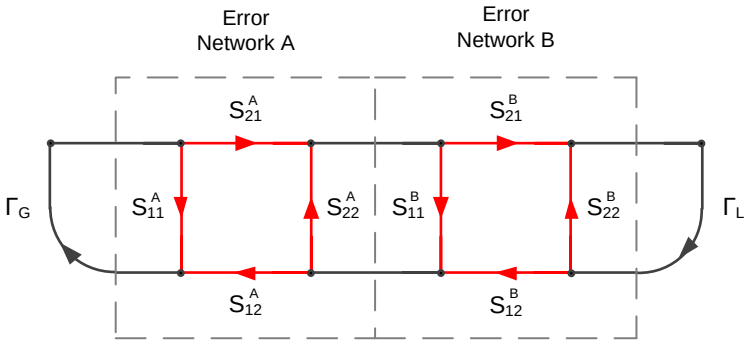

Figure 3.3. Signal flow diagram of a two sectioned two-port network.

$$\rho = \frac{+S_{21}S_{11}^{A}S_{12}\left(1-\left[S_{22}^{A}\Gamma_L\right]\right)+S_{21}S_{21}^{A}\Gamma_L S_{12}^{A}S_{12}}{1-\left[\left(S_{11}^{A}S_{22}\right)+\left(\Gamma_L S_{22}^{A}\right)+\left(S_{21}^{A}\Gamma_L S_{12}S_{22}\right)\right]+\left[S_{11}S_{22}S_{22}^{A}\Gamma_L\right]} \qquad (3.11)$$

$$S_{11}\left(1-\left[\left(S_{11}^{A}S_{22}\right)+\left(\Gamma_L S_{22}^{A}\right)+\left(S_{21}^{A}\Gamma_L S_{12}S_{22}\right)\right]+\left[S_{11}S_{22}S_{22}^{A}\Gamma_L\right]\right)$$

As with the single sectioned SFD network the source in figure 3.3 was assumed to be matched allowing equation (3.11) to be in a simplified form.

If the individual sections of figure 3.3 are representative of a pair of identical sections in a back-to-back configuration the following changes need be applied to equation (3.11),

(i) The input and output reflection coefficients of the second section are first exchanged, ($S_{11}^{A} \leftrightarrow S_{22}^{A}$), to ensure the network is in a back-to-back configuration. Since the two error networks are identical the respective input and

output reflection coefficients of the error networks can be made equal, ($S_{11}^A = S_{11}$) and ($S_{22}^A = S_{22}$).

(ii) The forward and reverse transmission coefficients of the second section are first exchanged, ($S_{12}^A \leftrightarrow S_{21}^A$), to ensure the network is in a back-to-back configuration. Since the two error networks are identical the respective forward and reverse transmission coefficients of the error networks can be made equal, ($S_{12}^A = S_{12}$) and ($S_{21}^A = S_{21}$).

(iii) The load is assumed to be matched, ($\Gamma_L = 0$).

The equation can be further simplified if reciprocity is applied. The resulting closed form equation, expressed by equation (3.12), is what is required to express a two-port Through measurement using an SFD model.

$$\rho = \frac{S_{11}\left(1 - {S_{22}}^2\right) + {S_{12}}^2 S_{22}}{1 - {S_{22}}^2} \tag{3.12}$$

Similar to the two sectioned SFD, a three sectioned SFD, such as the one shown in figure 2.2, presents many possible loop combinations. This again results in a complex general equation. Equation (3.13) is further simplified by assuming the source is matched.

By setting “error network A” identical to “error network B” the three sectioned SFD equation can be simplified. Furthermore, by placing the network in a back-to-back configuration similar changes, as those applied to the two sectioned SFD, can be applied to error networks of the three sectioned SFD. The second, or central section, is left unchanged and can be represent by either a Delay or Network electrical standard. The general SFD closed form equation describing a three sectioned network is given by

$$\rho = \frac{\begin{aligned} & S_{11}\left(1-\left[\left(S_{11}^{A}S_{22}\right)+\left(S_{11}^{B}S_{22}^{A}\right)+\left(S_{22}^{B}\Gamma_{L}\right)+\left(S_{21}^{A}S_{11}^{B}S_{12}^{A}S_{22}\right)\right.\right. \\ & \qquad \left.\left.+\left(S_{21}^{B}\Gamma_{L}S_{12}^{B}S_{22}^{A}\right)+\left(S_{21}^{A}S_{21}^{B}\Gamma_{L}S_{12}^{A}S_{12}^{B}S_{22}\right)\right] \\ & +\left[\left(S_{11}^{A}S_{22}\Gamma_{L}S_{22}^{B}\right)+\left(S_{11}^{A}S_{22}S_{11}^{B}S_{22}^{A}\right)+\left(S_{11}^{B}S_{22}^{A}\Gamma_{L}S_{22}^{B}\right)\right. \\ & \qquad \left.+\left(S_{11}^{A}S_{22}S_{21}^{B}\Gamma_{L}S_{12}^{B}S_{22}^{A}\right)+\left(\Gamma_{L}S_{22}^{B}S_{21}^{A}S_{11}^{B}S_{12}^{A}S_{22}\right)\right] \\ & -\left[\left(S_{11}^{A}S_{22}S_{11}^{B}S_{22}^{A}\Gamma_{L}S_{22}^{B}\right)\right]\Big) \\ & +S_{21}S_{11}^{A}S_{12}\left(1-\left[\left(S_{11}^{B}S_{22}^{A}\right)+\left(S_{22}^{B}\Gamma_{L}\right)\right]+\left[\left(S_{11}^{B}S_{22}^{A}\Gamma_{L}S_{22}^{B}\right)\right]\right) \\ & +S_{21}S_{21}^{A}S_{11}^{B}S_{12}^{A}S_{12}\left(1-\left[\left(S_{22}^{B}\Gamma_{L}\right)\right]\right) \\ & +S_{21}S_{21}^{A}S_{21}^{B}\Gamma_{L}S_{12}^{B}S_{12}^{A}S_{12} \end{aligned}}{\begin{aligned} & 1-\left[\left(S_{11}^{A}S_{22}\right)+\left(S_{11}^{B}S_{22}^{A}\right)+\left(S_{22}^{B}\Gamma_{L}\right)+\left(S_{21}^{A}S_{11}^{B}S_{12}^{A}S_{22}\right)\right. \\ & \qquad \left.+\left(S_{21}^{B}\Gamma_{L}S_{12}^{B}S_{22}^{A}\right)+\left(S_{21}^{A}S_{21}^{B}\Gamma_{L}S_{12}^{A}S_{12}^{B}S_{22}\right)\right] \\ & +\left[\left(S_{11}^{A}S_{22}\Gamma_{L}S_{22}^{B}\right)+\left(S_{11}^{A}S_{22}S_{11}^{B}S_{22}^{A}\right)+\left(S_{11}^{B}S_{22}^{A}\Gamma_{L}S_{22}^{B}\right)\right. \\ & \qquad \left.+\left(S_{11}^{A}S_{22}S_{21}^{B}\Gamma_{L}S_{12}^{B}S_{22}^{A}\right)+\left(\Gamma_{L}S_{22}^{B}S_{21}^{A}S_{11}^{B}S_{12}^{A}S_{22}\right)\right] \\ & -\left[\left(S_{11}^{A}S_{22}S_{11}^{B}S_{22}^{A}\Gamma_{L}S_{22}^{B}\right)\right] \end{aligned}} \quad . \qquad (3.13)$$

The closed form equation of a three sectioned network in a back-to-back configuration, where the two error networks are identical is expressed by

$$\rho = \frac{\begin{aligned} & S_{11}\left(1-\left[\left(S_{11}^{A}S_{22}\right)+\left(S_{22}^{B}S_{22}^{A}\right)+\left(S_{21}^{A}S_{22}^{B}S_{12}^{A}S_{22}\right)\right]+\left[\left(S_{11}^{A}S_{22}S_{22}^{B}S_{22}^{A}\right)\right]\right) \\ & +S_{21}S_{11}^{A}S_{12}\left(1-\left[\left(S_{22}^{B}S_{22}^{A}\right)\right]\right) \\ & +S_{21}S_{21}^{A}S_{11}^{B}S_{12}^{A}S_{12} \end{aligned}}{1-\left[\left(S_{11}^{A}S_{22}\right)+\left(S_{22}^{B}S_{22}^{A}\right)+\left(S_{21}^{A}S_{22}^{B}S_{12}^{A}S_{22}\right)\right]+\left[\left(S_{11}^{A}S_{22}S_{22}^{B}S_{22}^{A}\right)\right]} \qquad (3.14)$$

It is evident from the simplified equations formulated for the one, two and three sectioned SFD configurations that any of the three can be used to determine the network unknowns. The only condition that needs to be satisfied for de-embedding to be performed, discussed in Chapter 2, is that the three different reflection coefficient measurements need to be

performed using three unique electrical standards. In a back-to-back configuration the two sectioned SFD network can only represent a Through and therefore can only be used to obtain one of the three needed measurements. The other two measurements need be made using either of the remaining SFD configurations. The one and three sectioned SFD configurations can be used exclusively as long as the above electrical standard condition is satisfied.

A limitation of using a two and three sectioned SFD configuration is that in a back-to-back configuration a two-port measurement of the network needs to be performed. This is similar to the limitation observed for the cascade matrix method. However, unlike with the cascade matrix method, by terminating a single sectioned SFD in a Reflect electrical standard a one-port network is created which can be used exclusively to perform the network characterisation, as long as three unique measurements with three different Reflect terminations are performed. This is possible because the closed form equation derived for the single section SFD network contains all of the variables needed to describe a passive network.

The SFD method can also be used to characterise the reflection coefficient of an arbitrary load connected to a network. Once the properties of an error network have been characterised the reflection coefficient of an arbitrary load can be characterised by attaching it to the load terminal of the error network and performing a one-port measurement or calculations of the network. Thereafter, by applying equation (3.9) the reflection coefficient of the load can be isolated.

3.2.1 Three Offset Short De-embedding Method

The de-embedding method described in [13] makes use of a single section SFD network representation to describe the error network, which is then terminated in three offset short electrical standards. Each offset short is located at a different distance away from the error network load reference plane. The three resulting network configurations are shown in figure 3.4.

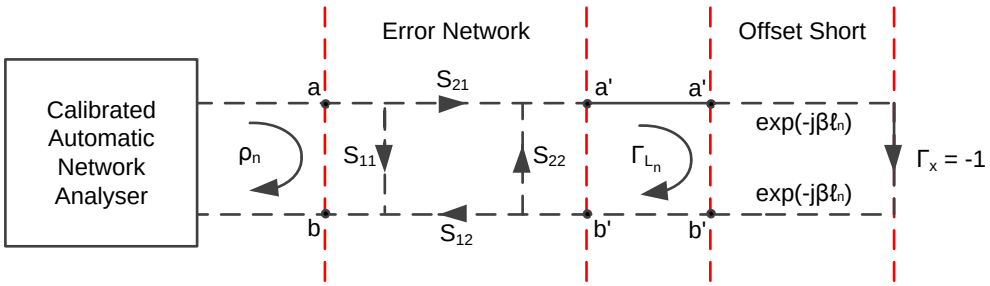

Figure 3.4. Error network terminated in three offset short electrical standards, with n = 1, 2 and 3.

The closed form equations corresponding to figure 3.4 are defined in [14] and the generic equation is given by

$$\rho_n = S_{11} + \frac{S_{12}S_{21}\Gamma_n}{1 - S_{22}\Gamma_n}\ , \tag{3.15}$$

and

$$\Gamma_n = \Gamma_x \exp\left[-2(\alpha + j\beta)l_n\right] \tag{3.16}$$

with n = 1, 2, 3 and where

ρ_n = reflection coefficient at the network terminal
Γ_n = reflection coefficient of the error network termination
Γ_x = reflection coefficient of the Short termination (Γ_x = -1)
l_n = distance between the network load reference plane and the termination
α = attenuation constant of the network
β = single mode propagation constant of the network.

The network was assumed to be lossless, thus allowing the attenuation constant to be set equal to zero.

From equation (3.16) it is evident that the three offset short de-embedding method allows for only one propagating mode to be treated at a time as only a solitary propagation constant can be defined. This allows the de-embedding method to be applied to characterising both TEM networks as well as a singular propagating mode of multi-modal networks. For this reason all further experiments using this de-embedding method were performed for the fundamental mode only.

The three equations, for the three different offset short terminations, were then simultaneously reworked in terms of the three unknown S-parameters of the error network and are given in equation (3.17) - (3.19).

$$S_{11} = \frac{\rho_1\rho_2\Gamma_3\left[\Gamma_2-\Gamma_1\right]+\rho_2\rho_3\Gamma_1\left[\Gamma_3-\Gamma_2\right]+\rho_1\rho_3\Gamma_2\left[\Gamma_1-\Gamma_3\right]}{\rho_1\Gamma_1\left[\Gamma_2-\Gamma_1\right]+\rho_2\Gamma_2\left[\Gamma_3-\Gamma_2\right]+\rho_3\Gamma_3\left[\Gamma_1-\Gamma_3\right]} \tag{3.17}$$

$$\begin{aligned} S_{22} &= \frac{S_{11}\left[\Gamma_2-\Gamma_1\right]+\rho_2\Gamma_1-\rho_1\Gamma_2}{\Gamma_1\Gamma_2\left[\rho_2-\rho_1\right]} \\ &= \frac{S_{11}\left[\Gamma_2-\Gamma_3\right]+\rho_2\Gamma_3-\rho_3\Gamma_2}{\Gamma_2\Gamma_3\left[\rho_2-\rho_3\right]} \end{aligned} \tag{3.18}$$

$$\begin{aligned} S_{12}S_{21} &= \frac{\left(\rho_1-S_{11}\right)\left(1-S_{22}\Gamma_1\right)}{\Gamma_1} \\ &= \frac{\left(\rho_2-S_{11}\right)\left(1-S_{22}\Gamma_2\right)}{\Gamma_2} \\ &= \frac{\left(\rho_3-S_{11}\right)\left(1-S_{22}\Gamma_3\right)}{\Gamma_3} \end{aligned} \tag{3.19}$$

Equation (3.19) returns the product of the forward and reverse transmission coefficients. The two transmission terms can be separated by taking the square-root of the product term. This is possible because the reciprocity principle was applied to the network making the two transmission terms equal.

3.2.2 Evaluation

To verify the efficacy of the three offset short de-embedding method for the purposes of network characterisation an experiment was devised. The first step is the implementation of equations (3.17) - (3.19) in a MATLAB algorithm. Secondly a test network is needed to serve as the error network with a known transfer function. This can then be evaluated by means of the software and compared to the known value. The input port of the test network is then designated the network terminal and the output port the device terminal.

For this purpose a lumped element third order Chebyshev lowpass filter was chosen. The lowpass filter was designed to have a cutoff frequency of 2.4 GHz and a passband ripple of 0.1 dB. The response of the designed filter is given in figure 3.5, obtained by simple ladder analysis into the matched ports.

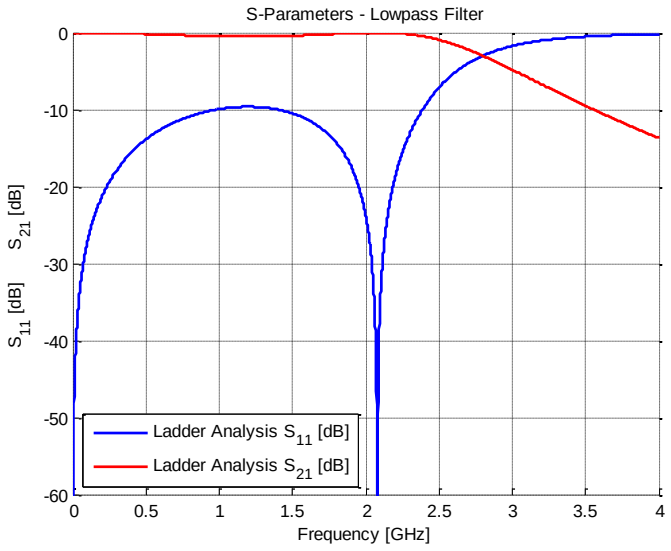

Figure 3.5. S-parameters of a 0.1 dB third order Chebyshev lowpass filter.

The device terminal of the lowpass filter was then terminated in three offset short electrical standards. The three offset lengths chosen for the de-embedding were $0\lambda_0$, $0.25\lambda_0$ and $0.5\lambda_0$, where λ_0 is the wavelength at the cutoff frequency. The phase responses of each of the three offset short measurements are shown in figure 3.6.

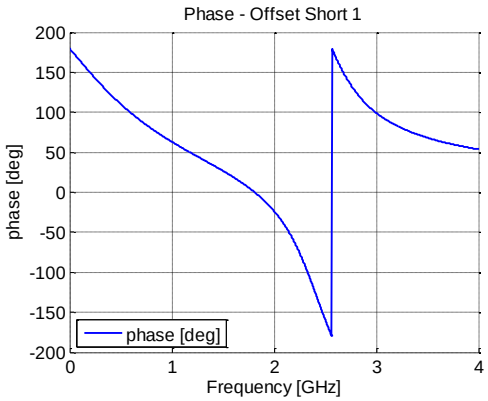

(a) Phase of $0\lambda_0$ offset short.

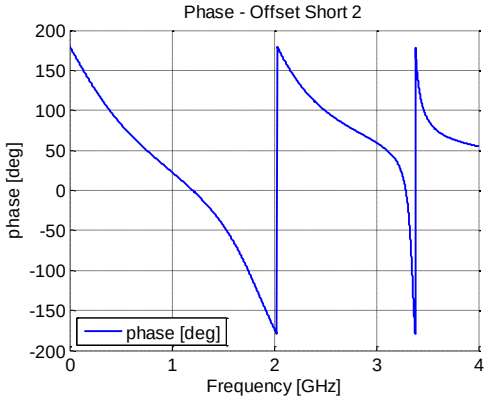

(b) Phase of $0.25\lambda_0$ offset short.

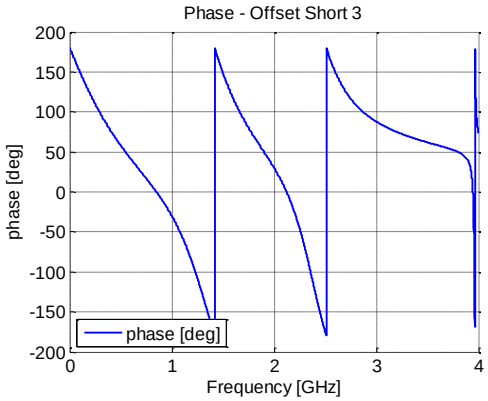

(c) Phase of $0.5\lambda_0$ offset short.

Figure 3.6. Phase responses of the three offset short terminations calculated for a lowpass filter test network.

The three offset short de-embedding method is principally hinged on the phase data of the individual measurements. The difference in phase together with the knowledge of the physical length of the offset and the propagation constant of the network are the fundamental parameters needed for this method to be usable for the purpose of network characterisation. The difference in phase between the three phase measurements in figure 3.6 are as a result of the offset of each measurement, which introduces an additional phase delay to the measurement.

The three offset short measurements were processed with the MATLAB algorithm and the characterised S-parameters of the error network, from 0 GHz – 4 GHz, are shown in figure 3.7.

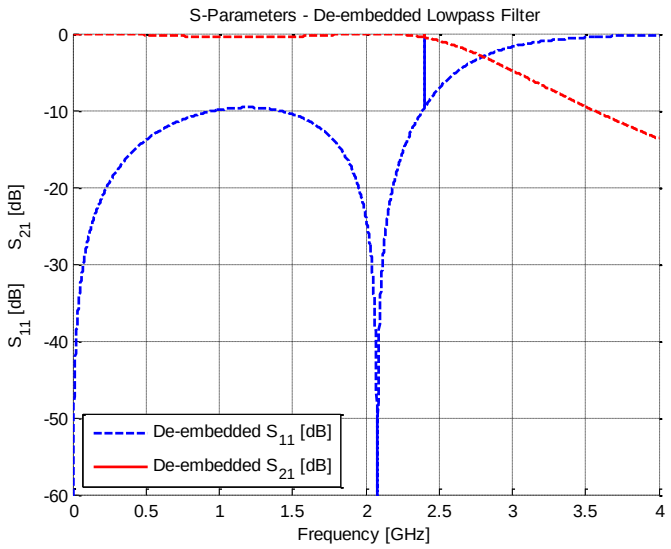

Figure 3.7. S-parameters of the third order lowpass filter error network calculated using the three offset short de-embedding method.

The de-embedded lowpass filter reflection and forward transmission response in figure 3.7 are for all intents and purposes identical to the lowpass filter reflection and forward transmission response in figure 3.5, which was obtained by means of a simple ladder analysis.

The singularity that occurs at 2.4 GHz in figure 3.7 is as a result of the offset lengths chosen for the characterisation process. At 2.4 GHz the $0.25\lambda_0$ offset short behaves like a quarter wavelength transformer, effectively presenting as an Open termination at the load reference plane of the error network. This is a limitation of this de-embedding method, as was pointed out in [48].

This limitation can be addressed in two different ways. The first is to replace the $0.25\lambda_0$ offset with a fourth offset short measurement made using a fourth different offset length. Thereafter proceed with the de-embedding method as previously described. This would result in the singularity occurring at a different frequency, related to the new offset length. By super-imposing the two calculated de-embedding results the occurrence of both singularities is removed. The second way is by careful choice of the initial three offset lengths. By choosing the offset lengths so that the quarter wavelength transformer occurs outside of the desired frequency range the occurrence of the singularities can be effectively removed.

3.2.3 De-embedding Application

Based on the performance of the MATLAB implemented three-Short de-embedding method on a lumped element lowpass filter the equations were implemented in a C++ based application. A screenshot of the application is shown in figure 3.8.

The application was written to have as user inputs the three measured reflection coefficient files, the physical lengths of the offsets and the cutoff frequency of the fundamental mode, which is dependent on the structure of the network. The output of the application is a text-file containing the de-embedded S-parameters of the error network and the corresponding frequency.

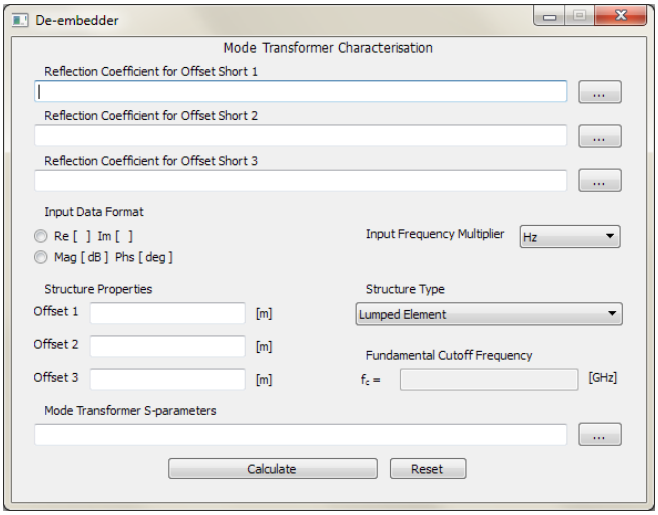

Figure 3.8. Screenshot of the C++ based de-embedding application implementing the three offset short de-embedding method.

The three offset short calculations were then processed in the C++ application. The comparison of the FEKO, MATLAB and C++ responses is shown in figure 3.9.

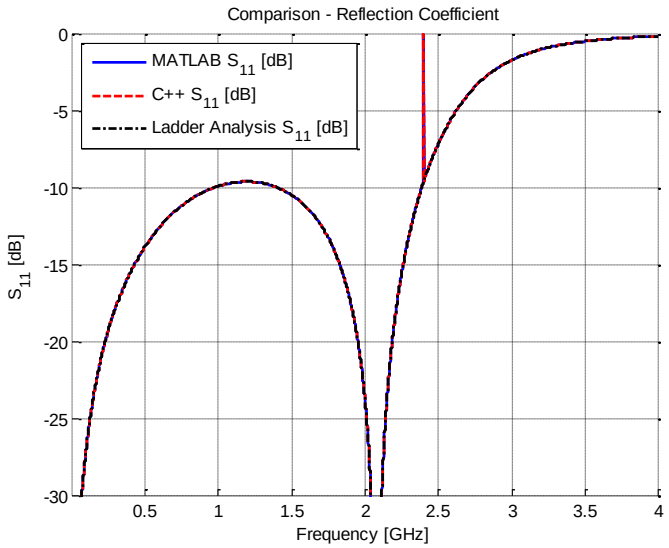

Figure 3.9. A comparison of the reflection coefficient of the lowpass filter network obtained from a ladder analysis, the MATLAB algorithm and the C++ application.

The characterised reflection coefficients from both the MATLAB algorithm and the C++ application are effectively identical to the reflection coefficient calculated by means of the ladder analysis. The difference between the error network characterisation and the ladder analysis reflection coefficient is due to the quarter wavelength resonances cause by the offset short terminations.

3.3 SUMMARY

Of the de-embedding methods discussed in Chapter 2 the analytically based class of de-embedding methods contains the Occum's Razor approach to de-embedding. Also, by not requiring the structural dimensions of the error network to be known for the purpose of characterisation, as is the case with the numerically based class of de-embedding methods, the analytically based class of de-embedding methods can be applied to the characterisation of any arbitrary network.

While the cascade matrix method and the SFD method are in many respects similar they do possess their individual attributes. The cascade matrix method presents a very convenient way of characterising the properties of a DUT which is embedded between two error networks; this under the condition that the properties of the embedding error networks are fully known. The SFD method presents both a convenient way of characterising a DUT embedded between two error networks as well as a way of easily characterising the properties of the error networks.

By making use of only the Delay and Short electrical standards the three offset short de-embedding method presents a very robust approach to performing network characterisation. This is partly due to the availability of the two electrical standards for a large number of microwave circuits and partly due to the ease with which the characterisation equations can be obtained.

The performance of the three offset short de-embedding method was verified by applying it to a test network, a lumped element lowpass filter. The reflection and transmission

properties of the test network, obtained by means of the three offset short de-embedding method, compared favourably to those calculated for the test network using a simple ladder analysis method. However, limitations of the three offset short characterisation method were observed. These presented as a singularity in the calculated S-parameters and were related to the choice of the offset lengths. By careful choice of these offsets the occurrence of the singularities can be made to show at frequencies outside the desired frequency range.

The robust nature of the SFD method, combined with the use of readily available electrical standards allows this de-embedding method to be applied to a large variety of different networks. In addition the error network characterisation equations were implemented in a C++ based application to make this characterisation method cross-platform accessible.

CHAPTER 4
CHARACTERISATION OF A PARALLEL LINE FEED MODEL

4.1 INTRODUCTION

A characterisation of a parallel line feed using the three offset short de-embedding method was performed. The implemented parallel line feed is similar to the one described in [49]. The structure was modelled in the full-wave EM simulation package FEKO. The MoM was chosen as the analysis method used to perform the simulations of the structure. The de-embedding was performed using the MATLAB algorithm as well as the C++ based application and the two sets of results are compared.

4.2 CHARACTERISATION OF A MODELLED PARALLEL LINE FEED

4.2.1 Characterisation of a Modelled Parallel Line Feed Using Three Offset Shorts

The dimensions of the parallel line feed used in this experiment were obtained from [49]. The feed lines are separated by a free space gap of 1.0 mm and the feed line width is 5.9 mm, which is for a 50 Ω characteristic impedance.

This was implemented in FEKO by making use of an infinitely large ground plane located equidistantly between the two feed lines. Applying image theory to the structure allows for one of the feed lines to be removed, effectively creating a microstrip line with a free space dielectric of 0.5 mm height. To ensure that the characteristic impedance of the parallel line feed structure remains 50 Ω, the effective microstrip characteristic impedance was defined as 25 Ω. A cross-sectional representation of the parallel line feed structure when using image theory is shown in figure 4.1.

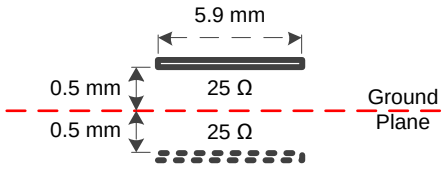

Figure 4.1. Cross-sectional view of a parallel line feed modelled using image theory.

The FEKO model of the microstrip line feed of length 66.7 mm which is located 0.5 mm above an infinitely large ground plane is shown in figure 4.2.

(a) **(b)**

Figure 4.2. Parallel line feed modelled as a microstrip line in FEKO showing an edge port (a) and a short termination (b).

As in [49] an edge port is placed at one end of the microstrip line, designated the network terminal. The other end of the microstrip line is terminated in three offset short terminations. The three offset lengths chosen for the experiment are 0 mm, 1.0 mm and 2.0 mm, respectively. The short terminations are modelled as a rectangular section of perfect electric conductor which connects the microstrip line to the ground plane. Three reflection coefficient measurements are performed at the edge port, one for each of the offset short terminations. The measurements are performed for 0 GHz – 42 GHz. The phase graphs of the three short termination measurements obtained from FEKO are shown in figure 4.3.

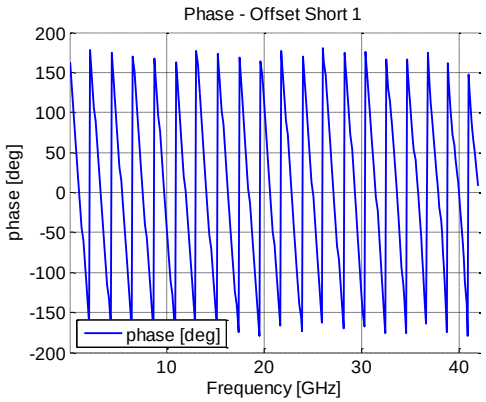

(a) Phase of 0 mm offset short.

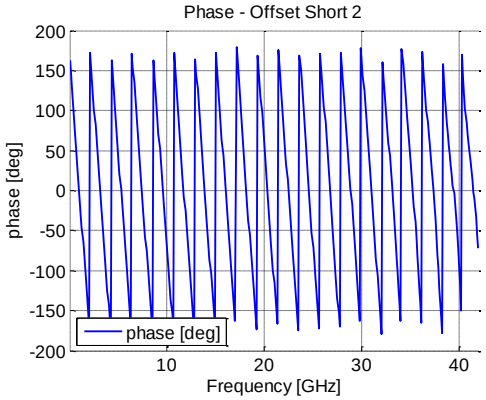

(b) Phase of 1 mm offset short.

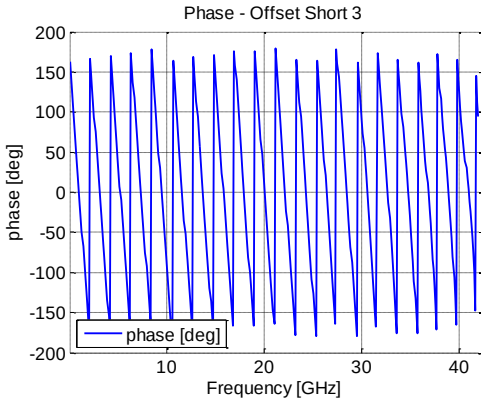

(c) Phase of 2 mm offset short.

Figure 4.3. Phase responses of the three offset short termination measurements of a parallel line feed.

A phase shift is observed between the three phase measurements in figure 4.3. This is caused by the offset lengths used in each measurement, which introduce an additional phase delay to the measurement.

The three offset short measurements were then imported into the MATLAB algorithm to perform the characterisation of the parallel line feed. The S-parameters of the characterised parallel line feed are shown in figure 4.4.

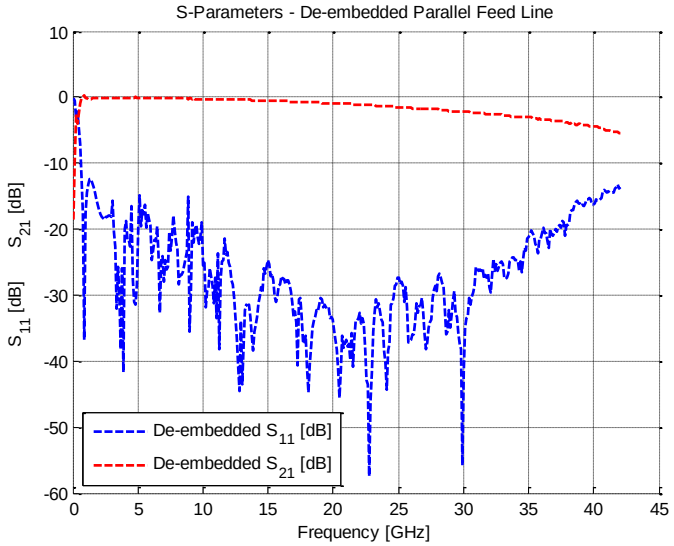

Figure 4.4. S-parameters of the parallel line feed error network characterised using the three offset short de-embedding method.

4.2.2 Two-port Reference Calculation

A fourth calculation of the microstrip line feed was needed to serve as a reference for the de-embedding procedure.

A second edge port was placed at the end of the line that was previously terminated in the Short electrical standards. A two-port characterisation of the microstrip line feed was performed in FEKO. The S-parameters of the de-embedded parallel line feed were then

compared to the S-parameters obtained for the two-port calculation. This comparison is shown in figure 4.5.

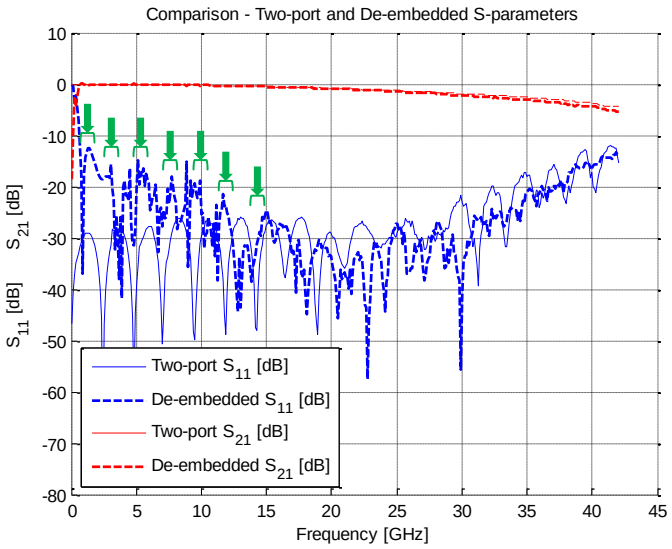

Figure 4.5. Comparison of the de-embedded and the two-port calculation S-parameters of the parallel line feed.

The singularities observed in the reflection coefficient of the lumped element test network in Chapter 3 are again observed in the parallel line feed network. The quarter wavelength transformer frequencies up to the 13^{th} quarter wavelength were calculated for the error network and offset lengths and are given in table 4.1. A correlation was observed between the calculated quarter wavelength transformer frequencies and the occurrence of the singularities in the S-parameters of the error network characterisation. This correlation is indicated with green arrows in figure 4.5.

An observation made in figure 4.5 is that the effect of the quarter wavelength transformer decreases for each quarter wavelength harmonic.

Table 4.1. Quarter wavelength transformer frequencies of the error network terminated in offset shorts.

Wavelength [$\lambda_{offset\ 1}$]	1/4	3/4	5/4	7/4	9/4	11/4	13/4
Frequency [GHz]	1.12	3.37	5.62	7.87	10.11	12.37	14.62

Wavelength [$\lambda_{offset\ 2}$]	1/4	3/4	5/4	7/4	9/4	11/4	13/4
Frequency [GHz]	1.11	3.32	5.54	7.75	9.97	12.19	14.40

Wavelength [$\lambda_{offset\ 3}$]	1/4	3/4	5/4	7/4	9/4	11/4	13/4
Frequency [GHz]	1.09	3.28	5.45	7.64	9.83	12.01	14.19

The three offset short calculations were then processed in the C++ application. The comparison of the two-port FEKO, MATLAB and C++ responses is shown in figure 4.6.

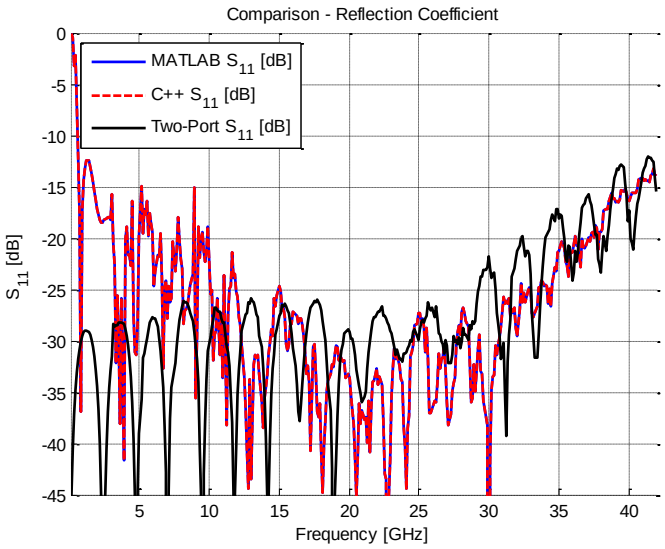

Figure 4.6. A comparison of the reflection coefficient of the parallel line feed obtained from FEKO, the MATLAB algorithm and the C++ application.

The characterised reflection coefficients from both the MATLAB algorithm and the C++ application are effectively identical. The difference between the error network

characterisation and the two-port FEKO reflection coefficient is due to the quarter wavelength resonances cause by the offset short terminations.

The VSWR of both the error network characterisation methods, when terminated in a matched load and that was calculated using the three offset short de-embedding method, are compared to the VSWR of the parallel line feed obtained from [49]. The comparison is shown in figure 4.7.

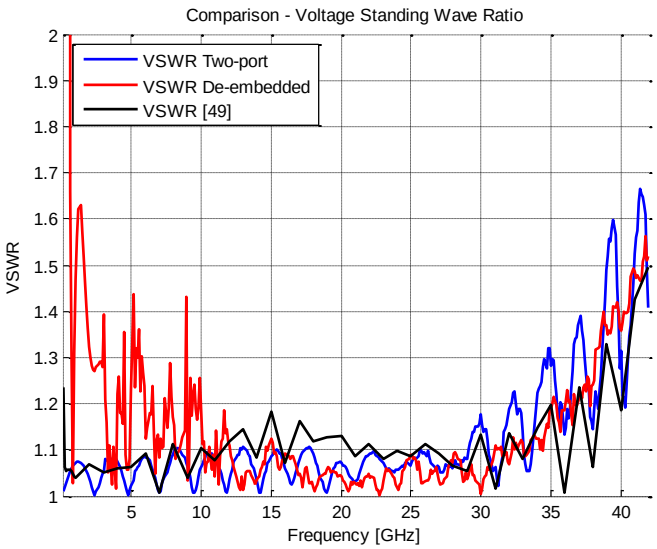

Figure 4.7. Comparison of the two-port FEKO VSWR, error network characterisation VSWR and the VSWR obtained from [49].

The VSWR calculated from the three offset short characterisation is in very good agreement with the two-port FEKO VSWR for the frequency range 10 GHz – 42 GHz. The difference between the two sets of VSWR that is observed between 0 GHz and 10 GHz occurs as a result of the effects of the quarter wavelength transformers. However, by careful choice of the offset lengths used the occurrence of the singularities can be made predictable. Thereafter by superimposing two sets of data the occurrence of the singularities can be eliminated.

To remove the effects of the singularities between 0 GHz and 10 GHz two additional sets of offset shorts were chosen. The first was chosen with a quarter wavelength at 4 GHz and the second with a quarter wavelength at 6 GHz. The three sets of data, from 0 GHz – 10 GHz and then from 10 GHz – 42 GHz, were superimposed and compared to the VSWR reported in [49]. This comparison is shown in figure 4.8.

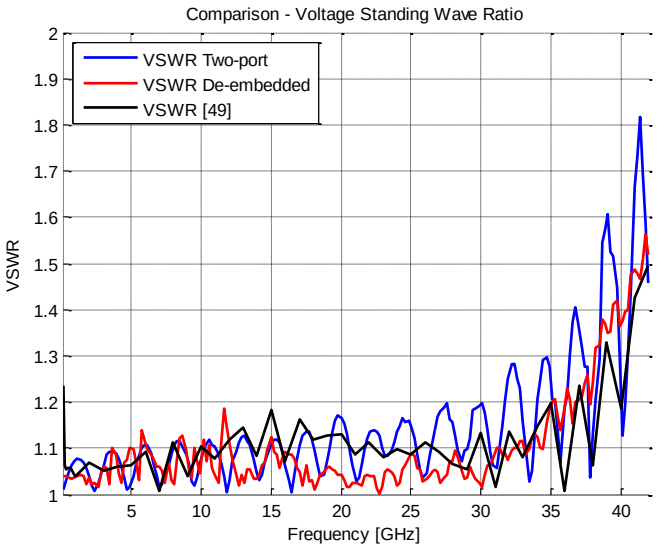

Figure 4.8. Comparison of the superimposed two-port FEKO VSWR, error network characterisation VSWR and the VSWR obtained from [49].

4.3 SUMMARY

A parallel line feed was modelled in FEKO and characterisation of the network was performed using the three offset short de-embedding method.

The parallel line feed was similar to the one used in [49]. The parallel line feed was modelled in FEKO as a microstrip line feed and by making use of an infinite ground plane image theory.

A two-port evaluation of the parallel line feed network was performed in FEKO to serve as a reference for the three offset short characterisation. The two sets of S-parameters compared favourably across the frequency range. However, the occurrence of singularities caused by quarter wavelength transformers was observed in the three offset short characterisation S-parameters.

Also calculated was the VSWR of the parallel line feed network. In the frequency range 10 GHz – 42 GHz both the VSWR obtained from the two-port FEKO evaluation and the VSWR obtained from the three offset short characterisation compared very well to the VSWR obtained from [49]. However, for the frequencies from 0 GHz – 10 GHz a notable difference in the VSWR is observed. This was as a result of the offset lengths chosen for the de-embedding procedure. By carefully choosing offset shorts the effects of the singularities were eliminated from the VSWR.

The three offset short de-embedding method presents an effective way of characterising a parallel line feed. The strengths of this de-embedding method are in that it only requires the use of Delay and Short electrical standards, which are well characterised and readily available for microstrip structures. It does however present inherent limitations related to the physical lengths.

CHAPTER 5
CHARACTERISATION OF A RECTANGULAR WAVEGUIDE MODE TRANSFORMER

5.1 INTRODUCTION

The characterisation of a coaxial to rectangular waveguide mode transformer using the three offset short de-embedding method was performed. This was carried out in two different ways. The physical X-band coaxial to rectangular waveguide mode transformer with an N-type to SMA adapter was evaluated on an HP 8510 ANA using three different offset shorts. The S-parameters of the three offset short terminations were processed using both the MATLAB and C++ algorithms. These results were verified by creating a CAD model of the mode transformer in FEKO, and evaluating it by means of MoM.

5.2 CHARACTERISATION OF A PHYSICAL X-BAND COAXIAL TO RECTANGULAR WAVEGUIDE MODE TRANSFORMER

5.2.1 Characterisation of a Sivers Lab PM 7325X X-band Coaxial to Rectangular Waveguide Mode Transformer Using Three Offset Shorts

A Sivers Lab PM 7325X X-band coaxial to rectangular waveguide mode transformer with an N-type to SMA adapter is shown in figure 5.1.

Figure 5.1. Sivers Lab PM 7325X X-band mode transformer with an N-type to SMA adapter.

Two X-band delay plates were available for the experiment, which meant that the three offset shorts were located at 0 mm, 5.0 mm and 14.8 mm away from the mode transformer load reference plane. A photo of the two delay plates together with the Short plate are shown in figure 5.2.

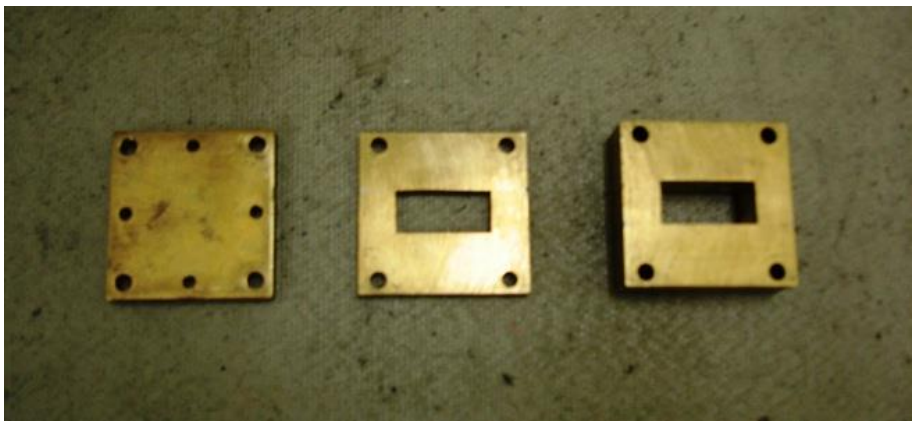

Figure 5.2. Two X-band delay plates together with the Short plate used for the experiment.

The three measurements were performed over the 5 GHz – 15 GHz frequency range and the phase graphs of each measured reflection coefficient are shown in figure 5.3.

A phase shift is observed between the three phase measurements, shown in figure 5.3. This is caused by the offset lengths used in each measurement, which introduce an additional phase delay to the measurement.

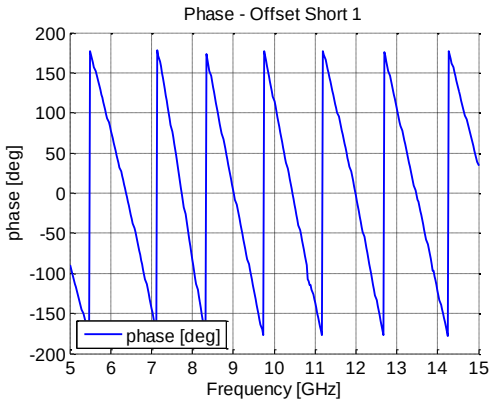

(a) Phase of 0 mm offset short.

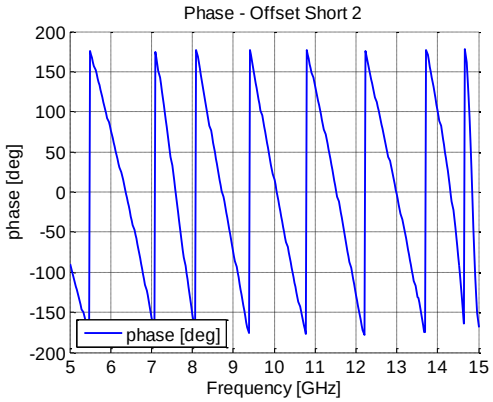

(b) Phase of 5 mm offset short.

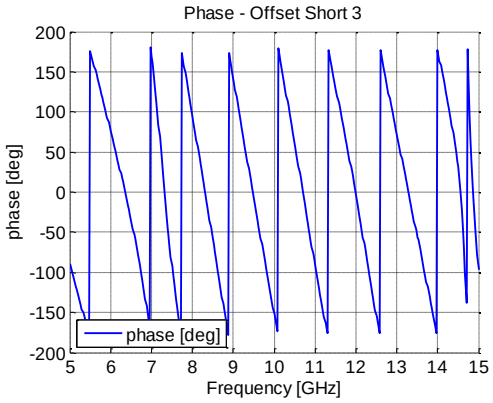

(c) Phase of 14.8 mm offset short.

Figure 5.3. Phase responses of the three offset short termination measurements of a Sivers Lab PM 7325X X-band mode transformer with an N-type to SMA adapter.

The three reflection coefficient measurements were processed using the MATLAB algorithm and the resulting forward reflection and transmission coefficients are shown in figure 5.4.

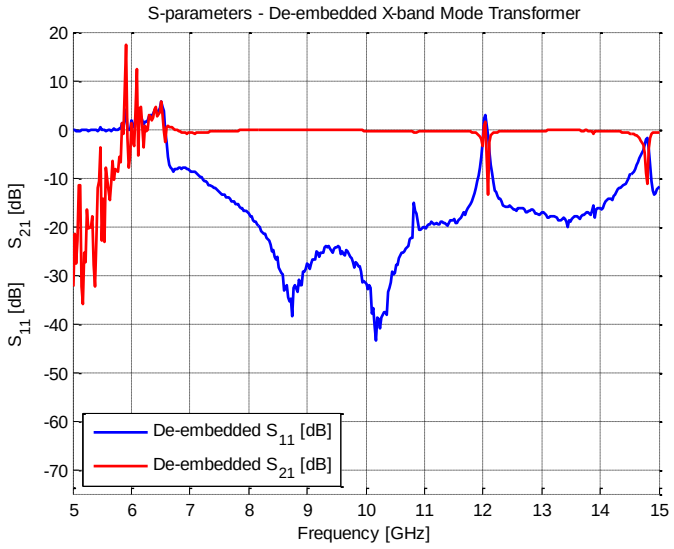

Figure 5.4. S-parameters of an X-band mode transformer characterised using the three offset short de-embedding method.

5.2.2 Two-port Reference Calculation

A fourth measurement of the X-band mode transformer was performed by terminating it in a rectangular waveguide matched load standard. The matched load was placed at the load reference plane of the mode transformer. The measurement using the matched load was conducted to serve as a reference response for the performance of the mode transformer. By assuming that the system is lossless the forward transmission coefficient was calculated from the conservation of energy principle as is described by

$$|S_{11}|^2 + |S_{21}|^2 = 1 \ . \tag{5.1}$$

The S-parameters of the three offset short characterisation method were then compared directly against the matched load reference measurement. This comparison is shown in figure 5.5.

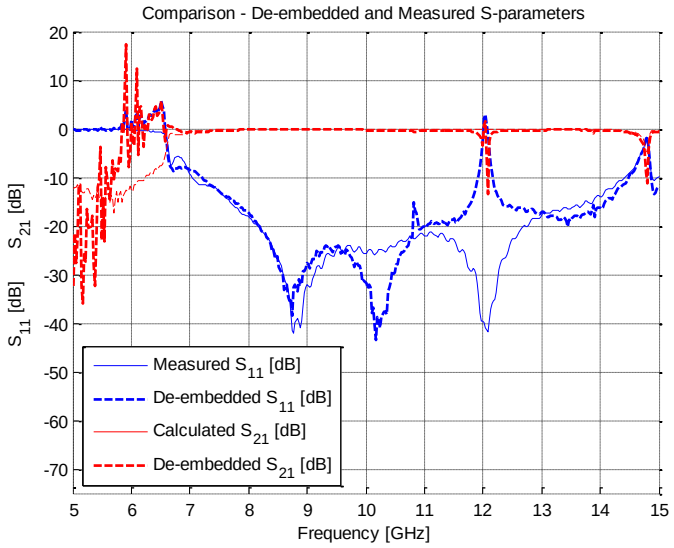

Figure 5.5. Comparison of de-embedded and measured S-parameters of the X-band mode transformer.

For frequencies below approximately 6.5 GHz the mode transformer is operating below the fundamental cutoff frequency, as was calculated by

$$f_{c_{mn}} = \frac{1}{2\sqrt{\mu\varepsilon}}\sqrt{\left(\frac{m}{a}\right)^2 + \left(\frac{n}{b}\right)^2} \quad . \tag{5.2}$$

For frequencies below the fundamental cutoff frequency the propagation constant is imaginary thus causing the erroneous characterisation properties to be calculated.

In the 6.5 GHz – 11.5 GHz frequency range the reflection coefficient of the mode transformer obtained by means of the three short characterisation compares well to the reflection coefficient measurement obtained using a matched load termination. However, for frequencies between 11.5 GHz and 12.5 GHz a difference is observed between the de-embedded and measured reflection coefficient.

This could be as a result of two things. The first possible cause of the difference is the presence of high order modes propagating along the waveguide. This was investigated by

determining the cutoff frequency of the higher propagating modes using equation (5.2). The next mode is TE_{20} which has a cutoff frequency of 13.12 GHz. It can therefore not be the cause of the difference occurring at 12.1 GHz.

The second possible cause of the difference is that one of the offset short terminations is a quarter wavelength, or an odd multiple of a quarter wavelength, away from the pin location. This will cause the structure effectively behaving like a quarter wavelength transformer at that particular frequency. The wavelength of a wave travelling inside a waveguide is determined using

$$\lambda_g = \frac{\lambda}{\sqrt{1-\left(\frac{\lambda}{\lambda_c}\right)^2}} = \frac{c/f}{\sqrt{1-\left(\frac{c/f}{2a}\right)^2}} \,. \tag{5.3}$$

Using equation (5.3), [50], the quarter wavelength at 12.1 GHz is calculated to be 7.4 mm and the three-quarter wavelength was found to be 22.2 mm. The three quarter wavelength corresponds very well to the distance between the centre of the mode transformer pin and the location of the first short termination, as is shown in figure 5.6.

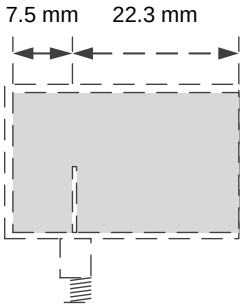

Figure 5.6. Cross-section of a coaxial to rectangular waveguide mode transformer showing the distance between the centre of the pin and both the backshort and the first short termination.

Also shown in figure 5.6 is the distance between the centre of the mode transformer pin and the backshort. This distance was measured to be 7.5 mm, which is approximately a

quarter wavelength at 12.1 GHz. Since the distance between the pin and backshort does not change throughout the experiment the influence of the quarter wavelength transformer formed by the backshort will be present in all of the offset short measurements. Combining this with the influence of the three-quarter wave transformer formed by the first offset short describes the difference observed at approximately 12.1 GHz. This difference is similar to the singularity observed for the ideal lowpass filter characterisation in section 3.2.1.

The three offset short measurements performed using an ANA were then processed in the C++ application. The comparison of the ANA, MATLAB and C++ reflection coefficient is shown in figure 5.7.

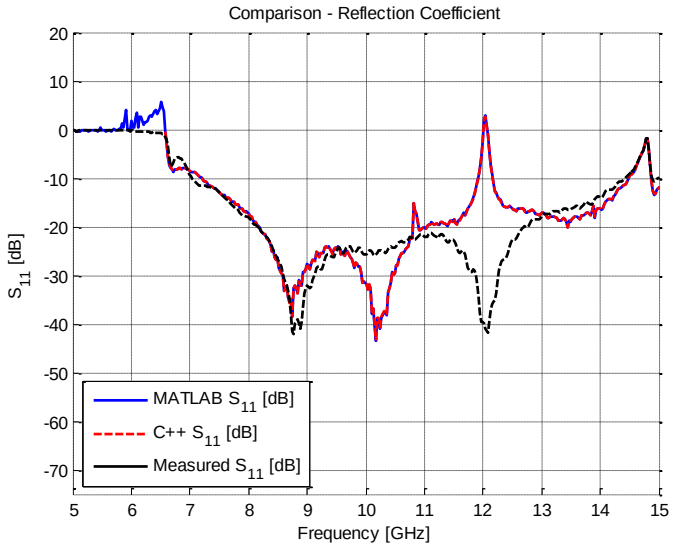

Figure 5.7. A comparison of the reflection coefficient of the mode transformer obtained from an ANA Measurement, the MATLAB algorithm and the C++ application.

Both of the three offset short characterised reflection coefficients, one obtained from the MATLAB algorithm and the other from the C++ application, are effectively identical and both compare favourably to the reflection coefficient obtained from the ANA matched load measurement.

5.3 CHARACTERISATION OF A MODELLED X-BAND COAXIAL TO RECTANGULAR WAVEGUIDE MODE TRANSFORMER

5.3.1 Characterisation of a Modelled X-band Coaxial to Rectangular Waveguide Mode Transformer Using Three Offset Shorts

Measurements were taken of the mode transformer used in the physical experiment and the structure was modelled in FEKO. The FEKO model of the mode transformer is shown in figure 5.8.

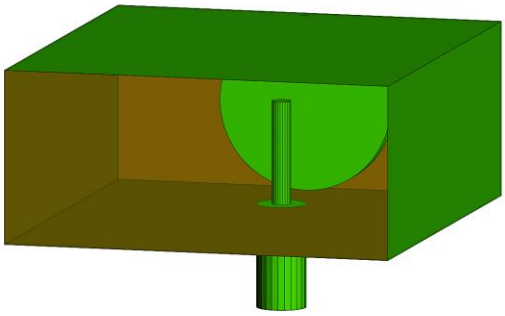

Figure 5.8. FEKO model of X-band coaxial to rectangular waveguide mode transformer.

The dimensions of the structure are fixed; the only aspect of the model that required defining was the way of modelling the coaxial line and pin of the mode transformer.

Two possible coaxial line models were considered. The first was to use a very thin wire as an approximation of the centre conductor of the coaxial line. This is driven using a delta-gap excitation source located at the centre of the wire. This model is very easy to implement but may be an over-simplified way of addressing the coaxial to waveguide transition. The second, more complex, method is to model the coaxial line as a coaxial waveguide.

The characteristic impedance of the coaxial waveguide was chosen to be 50 Ω, to match the characteristic impedance of the standard transmission line. The coaxial waveguide was filled with a dielectric, of relative permittivity of 2.2, to more closely model the coaxial

transmission lines used in the physical experiment. The dimensions for a dielectric filled coaxial waveguide with relative permittivity of 2.2 were calculated as

$$Z_0 = \frac{1}{2\pi}\sqrt{\frac{\mu}{\varepsilon}}\ln\left(\frac{D}{d}\right), \tag{5.4}$$

where

D = outer diameter of coaxial waveguide
d = inner diameter of coaxial waveguide.

Choosing D = 2.9 mm and d = 0.9 mm results in a characteristic impedance of 47.30 Ω, which is an acceptable approximation to the chosen characteristic impedance.

The coaxial waveguide was initially modelled as two concentric metal cylinders. However, when meshing of these structures is done in FEKO the resulting mesh is inhomogeneous along the length of the coaxial waveguide geometry. This can be adequately addressed by approximating the circularity of the cylinders with a 24-sided polygon. This creates a geometry that is meshed homogeneously along the length of the geometry. A comparison of the mesh of a 24-sided and circular coaxial waveguide structure is shown in figure 5.9.

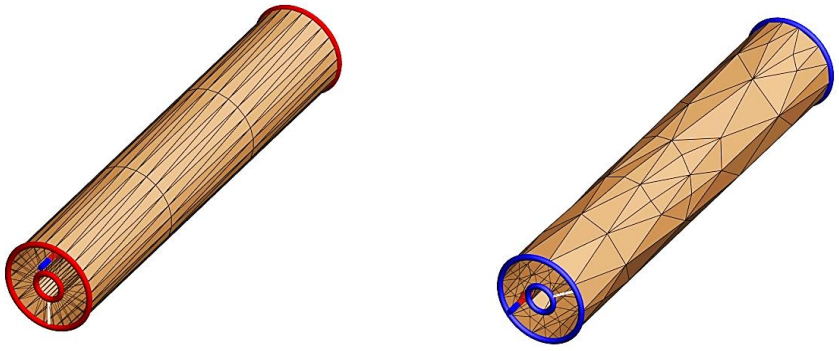

Figure 5.9. Model mesh of a 24-sided (left) and circular (right) coaxial waveguide structure.

(a) Phase of 0 mm offset short.

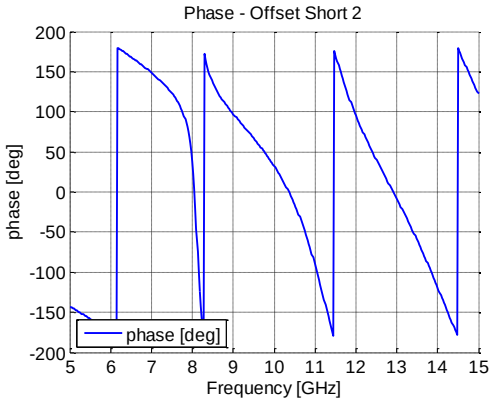

(b) Phase of 5 mm offset short.

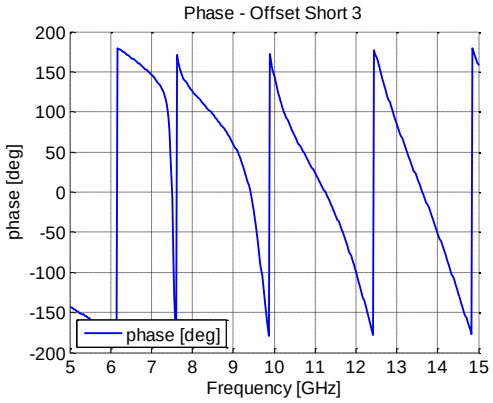

(c) Phase of 14.8 mm offset short.

Figure 5.10. Phase responses of the three offset short termination measurements of an X-band mode transformer model.

A waveguide port was placed at the base of the coaxial waveguide and a TEM source was defined for that port. The rectangular waveguide then terminated in three offset short plates of the same length as those available for the physical structure. The phase graphs for the three short terminations obtained from FEKO are shown in figure 5.10.

A phase shift is observed between the three phase measurements. This is caused by the offset lengths used in each measurement, which introduce an additional phase delay to the measurement.

The three offset short measurements were then processed in the MATLAB. The waveguide propagation constant for the fundamental mode, required for the de-embedding algorithm, was calculated using

$$\beta_g = \frac{2\pi f}{c} \frac{1}{\sqrt{1-\left(\frac{f_c}{f}\right)^2}} \ . \tag{5.5}$$

5.3.2 Two-port Reference Calculation

A fourth calculation of the structure was needed to serve as a reference for the de-embedding procedure. A FEKO waveguide port was placed at the aperture of the rectangular waveguide; a fundamental mode source was defined for this port. Then, a two-port characterisation of the mode transformer was performed in FEKO. The S-parameters of the mode transformer characterised by means of the three offset short method were then compared to the S-parameters obtained for the two-port calculation. The comparison is shown in figure 5.11.

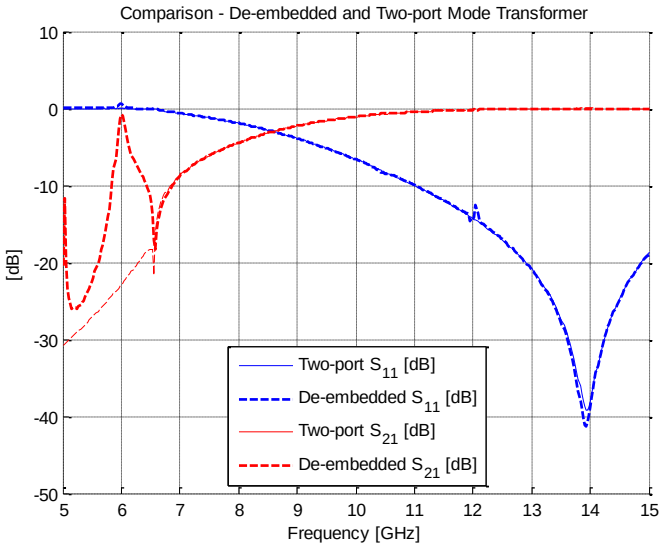

Figure 5.11. Comparison of the de-embedded and the two-port measurement reflection and transmission responses of the coaxial to rectangular waveguide mode transformer.

The S-parameters obtained by means of the three offset short method compare favourably to the S-parameters obtained from the two-port FEKO calculation of the mode transformer.

In the de-embedded results a difference is observed at approximately 12.1 GHz. This is consistent with the difference observed for the physical structure and is as a result of the backshort being located a quarter wavelength away from the coaxial pin. A further influence on the deviation is that the first offset short termination is three-quarter wavelengths away from the coaxial pin, effectively behaving like a quarter wavelength transformer.

The three offset short measurements were then processed in the C++ application. The comparison of the FEKO, MATLAB and C++ responses is shown in figure 5.12.

The characterised reflection coefficients from both the MATLAB algorithm and the C++ application are in very good agreement. The difference between them is as a result of a difference in numerical accuracy of the respective applications. The difference between the de-embedded characterisation and the two-port FEKO reflection coefficient is due to the

quarter wavelength resonances cause by the offset short terminations. The C++ derived reflection coefficient exhibits the same deviation at 12.1 GHz as previously discussed.

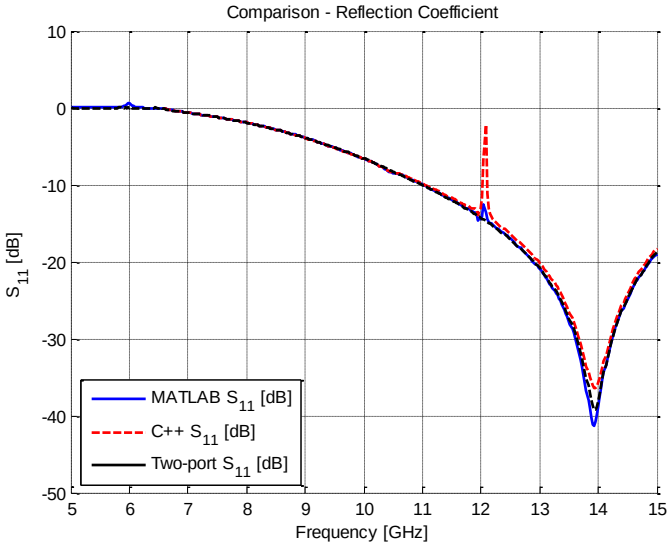

Figure 5.12. A comparison of the reflection coefficient of the mode transformer obtained from FEKO, the MATLAB algorithm and the C++ application.

5.4 SUMMARY

The three offset short de-embedding method was applied to characterising the properties of a coaxial to rectangular waveguide mode transformer.

Firstly the de-embedding method was applied to a Sivers Lab PM 7325X X-band mode transformer. The mode transformer was terminated in a matched load and the results of this measurement were used as a reference for the performance of the mode transformer. The mode transformer S-parameters obtained by means of the three offset short method were compared to a matched load measurement. Apart from the difference that was observed at 12.1 GHz the three offset short method S-parameters were in good agreement with those obtained from the matched load measurement. The aforementioned difference was as a result of the backshort, which at 12.1 GHz is located a quarter of a wavelength away from the pin of the mode transformer.

Secondly a CAD model of the Sivers Lab PM 7325X was created in FEKO and the three offset short de-embedding method was applied to this model. As a reference measurement the model was terminated in a second waveguide port at the aperture of the waveguide and a two-port measurement was made. The S-parameters of the three offset short de-embedding method were in good agreement with those obtained from the two-port measurement of the mode transformer in FEKO. As observed for the physical structure the three offset short S-parameters of the FEKO model also show a difference at 12.1 GHz. As with the physical mode transformer, the backshort was located approximately a quarter of a wavelength away from the pin and at 12.1 GHz this presented as a quarter wavelength transformer.

The three offset short de-embedding method presents an effective way of characterising a coaxial to rectangular waveguide mode transformer. The strength of this de-embedding method is in that it only requires the use of Delay and Short electrical standards, which are well characterised and readily available for rectangular waveguide structures. It does however have inherent limitations related to the internal lengths. These can, for the most part, be addressed by careful choice of the offset lengths. However, for coaxial to waveguide mode transformers the delay between the pin and the backshort may present a quarter wavelength transformer in the desired characterisation frequency range. This can be addressed by moving the backshort closer to the pin thus decreasing the distance and subsequently shifting the quarter wavelength transformer to occur at a higher frequency, preferably outside the workable frequency range of the mode transformer. This was tested for the coaxial to double ridged waveguide mode transformer shown in Chapter 6.

CHAPTER 6

CHARACTERISATION OF A DOUBLE RIDGED WAVEGUIDE MODE TRANSFORMER

6.1 INTRODUCTION

The design and then characterisation of a coaxial to double ridged waveguide mode transformer, using the three offset short de-embedding method, was performed. The structure was based on the X-band mode transformer discussed in Chapter 5. The designed model was implemented in the full wave EM simulation package FEKO. This presented with a problem as the waveguide ports available in FEKO cannot be placed on a face that contains metal surfaces. Consequently, the presence of any ridge faces at the aperture of the waveguide port will result in simulation errors. A way of addressing this problem is to define a dielectric material with the same properties as free space and then fill all the regions that are to be air inside the structure with this dielectric. This allows for a Finite Element Method (FEM) Modal port to be placed at the aperture of the mode transformer thus allowing the model to be simulated. The waveguide ports generally used in FEKO were thus substituted with FEM Modal ports. The final step is to define the simulator to perform an FEM simulation instead of the usual MoM simulation. The accuracy of this method was tested by the manufacturers of FEKO on a waveguide step model and it was show to be comparable to the accuracy obtained from an MoM simulation [51].

6.2 DOUBLE RIDGED WAVEGUIDE STRUCTURE DESIGN

The dimensions of the X-band rectangular waveguide, discussed in Chapter 5, were used as a basis for the double ridged waveguide structure. The ridges of the latter were designed following the guidelines set out by Hopfer [52] and Cohn [53]. The longitudinal dimensions of the model were chosen to be symmetrical and the top and bottom ridges were chosen to be identical. The lower dimensional limit of the ridge width was set by the outer diameter of the coaxial waveguide. Thereafter a parametric study on the ridge

dimensions was performed to optimise the transmission properties of the mode transformer so that it exhibited a centre frequency at 10 GHz.

A rectangular cavity was defined at the back of the mode transformer and the backshort was placed 3 mm behind the back face of the ridges. The ridge length was chosen to be 15 mm from the back face of the ridges. The centre of the coaxial waveguide, which formed the mode transformer pin, was located 2.5 mm from the back face of the ridges.

The coaxial waveguide model was obtained in the same way as for the rectangular waveguide structure, as described in section 5.3. The only difference was that the outer cylinder was extended to the top face of the bottom ridge. The inner cylinder was further extended to touch the bottom face of the top ridge, thus spanning the gap between and the two ridges and subsequently creating the mode transformer pin.

A cross-sectional diagram of the designed coaxial to double ridged waveguide mode transformer is shown in figure 6.1.

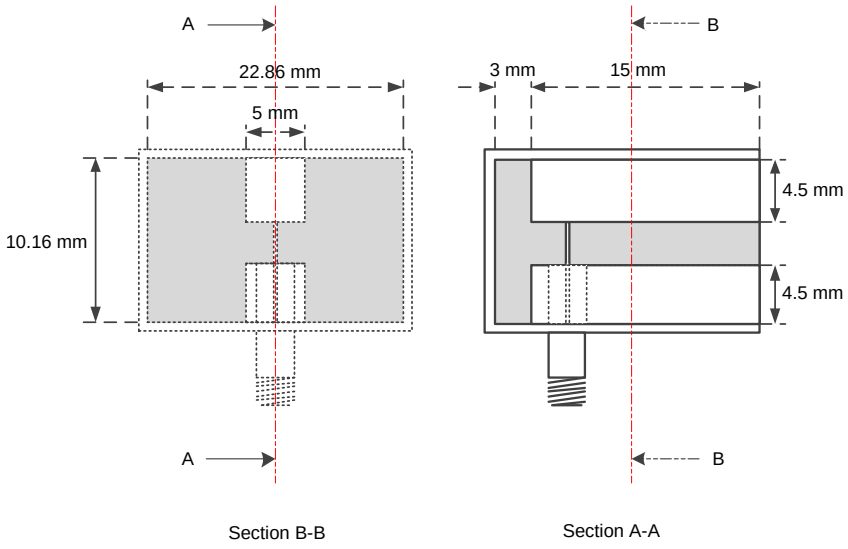

Figure 6.1. Cross-sectional diagram of coaxial to double ridged waveguide mode transformer.

6.3 CHARACTERISATION OF A DOUBLE RIDGED WAVEGUIDE MODE TRANSFORMER

6.3.1 Characterisation of a Coaxial to Double Ridged Waveguide Mode Transformer Using Three Offset Shorts

The designed coaxial to double ridge waveguide mode transformer was modelled in FEKO. The FEKO model is shown in figure 6.2.

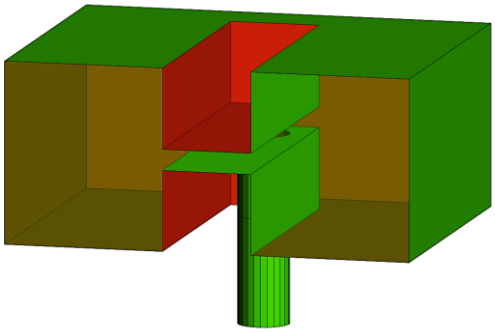

Figure 6.2. FEKO model of coaxial to double ridge waveguide mode transformer.

The free space regions of the model were replaced by a dielectric material with the same properties as free space. The simulator was configured to perform an FEM simulation of the model as opposed to the MoM simulation usually used for waveguide models. As a result the waveguide ports used for the simulation of rectangular waveguide model also needed to be replaced, with FEM modal ports. An FEM modal port was placed at the base of the coaxial waveguide.

The three offset lengths used for this model were 0 mm, 5 mm and 10 mm. The first short plate was placed at the aperture of the ridged waveguide; for the other two offset short terminations the waveguide and ridges were extended by the chosen offset length and the short plate was placed at the end of the extension. The phase graphs of the three offset terminations are shown in figure 6.3.

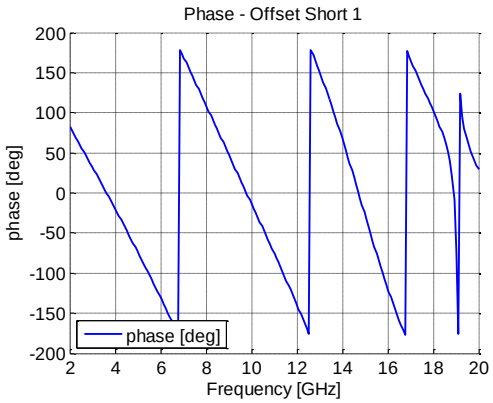

(a) Phase of 0 mm offset short.

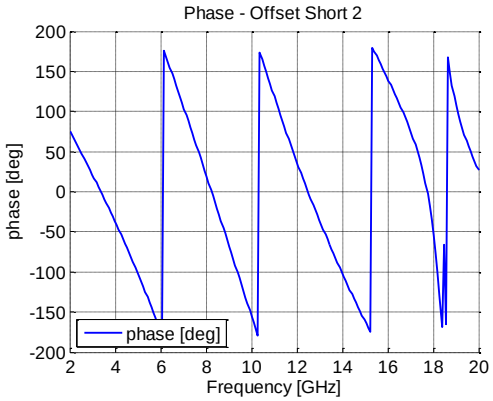

(b) Phase of 5 mm offset short.

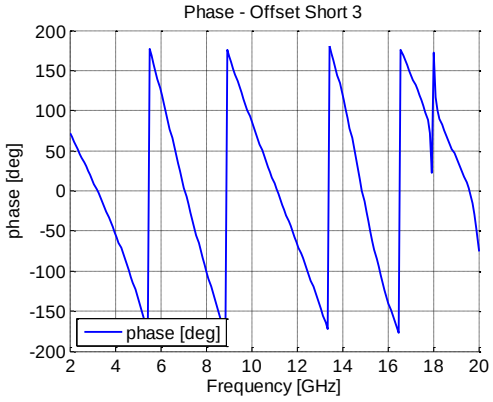

(c) Phase of 10 mm offset short.

Figure 6.3. Phase responses of the three offset short termination measurements of a double ridged waveguide mode transformer model.

A phase shift is observed between the three phase measurements in figure 6.3. This is caused by the offset lengths used in each measurement, which introduce an additional phase delay to the measurement. Also, discontinuities in the phase are identified at approximately 18 GHz, 18.5 GHz and 19 GHz. These are discussed later in this chapter.

The three offset short measurements were then imported into the MATLAB algorithm to perform the de-embedding of the mode transformer. The S-parameters of the de-embedded mode transformer are shown in figure 6.4.

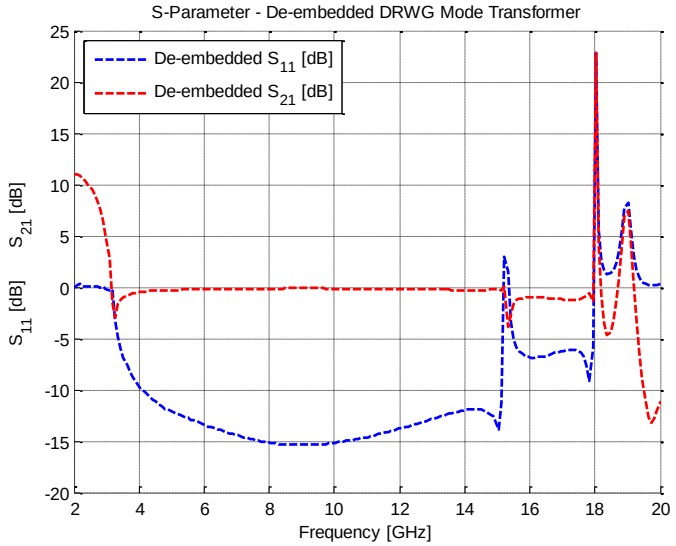

Figure 6.4. De-embedded reflection and transmission responses of the coaxial to double ridged waveguide mode transformer.

For frequencies below approximately 3.2 GHz the mode transformer is operating below the fundamental cutoff frequency, as was determined from [52]. For frequencies below the fundamental cutoff frequency the propagation constant is imaginary thus causing the erroneous characterisation properties to be calculated.

6.3.2 Two-port Reference Calculation

A fourth calculation of the model was needed to serve as a reference for the de-embedding procedure. A FEM modal port was placed at the aperture of the ridged waveguide, and a fundamental mode source was defined for this port. Then, similar to a matched load measurement of the physical structure, a two-port characterisation of the mode transformer was performed in FEKO over the 2 GHz – 20 GHz frequency range. The S-parameters of the de-embedded mode transformer were then compared to the results obtained for the two-port calculation. The comparison is shown in figure 6.5.

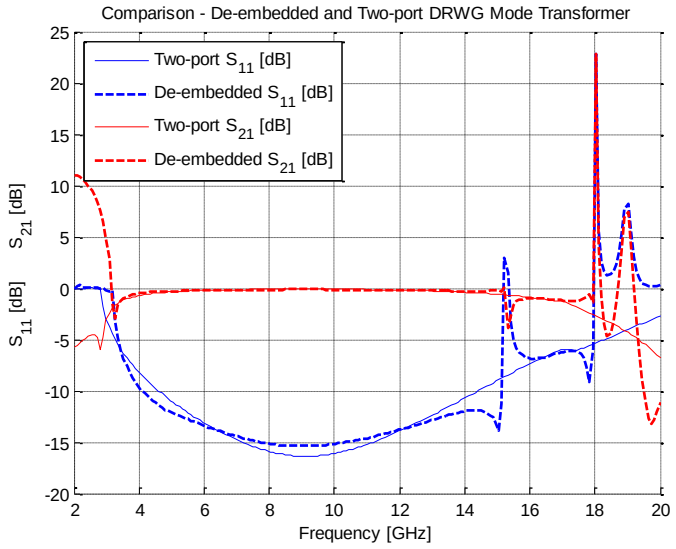

Figure 6.5. Comparison of the de-embedded and the two-port measurement reflection and transmission responses of the coaxial to double ridged waveguide mode transformer.

The cutoff frequencies of the TE_{10}, TE_{20} and TE_{30} modes were determined from [52] and were found to be 3.20 GHz, 15.26 GHz and 16.83 GHz, respectively. The cutoff frequency of the TE_{10} mode was used in equation (5.5) to determine the fundamental mode propagation constant of the waveguide.

The performance of the de-embedded structure is as expected for frequencies up to approximately 15 GHz as it is in good agreement with the results obtained for the two-port

structure. However, at approximately 15.5 GHz, 18 GHz and 19 GHz singularities are observed in the de-embedded results.

The singularity at approximately 15.5 GHz corresponds to a quarter wavelength of 5.35 mm, which is the approximate distance between the centre of the mode transformer pin and the backshort. Furthermore, it is influenced by the three quarter wavelength transformer that is formed between the centre of the mode transformer pin and the second offset short termination. Similarly the singularity at approximately 19 GHz corresponds to a three-quarter wavelength transformer length of 12.6 mm, which is formed when using the first offset short termination. These observations are consistent with those made for the coaxial to rectangular waveguide mode transformer.

The singularity at 18 GHz does not correspond to any immediately obvious lengths inside the model that may form a quarter wavelength transformer. It does however occur above the cutoff frequency of the next higher order mode and could thus occur as a result of higher order mode propagation.

6.3.3 Eliminating the Singularities

In an endeavour to address the matter of the singularities the effects that the structural dimensions of the network have on the occurrence of the singularities were investigated. Consequently, the lengths between the mode transformer pin and both the backshort and offset shorts need to be changed. This is be done by shifting the waveguide reference plane and the backshort closer to the mode transformer pin, subsequently altering the dimensions of the mode transformer model. The backshort was moved closer to the mode transformer pin, reducing the length from 3 mm to 2.5 mm, and the length between the mode transformer pin and the aperture of the ridged waveguide from 15 mm to 7 mm. The lengths of the three offset shorts were also made shorter, namely 0 mm, 1 mm and 2 mm, respectively. The shortened double ridged waveguide structure is shown in figure 6.6.

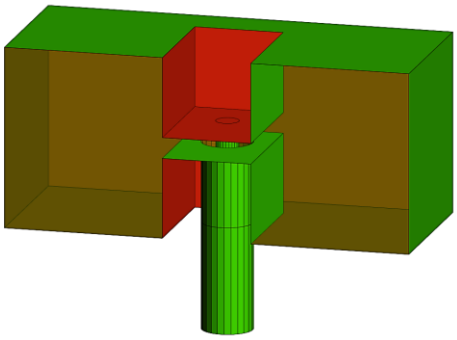

Figure 6.6. FEKO model of the shortened coaxial to double ridge waveguide mode transformer.

As before a two-port structure was defined and simulated in FEKO to serve as a reference for the reflection and transmission properties of the mode transformer.

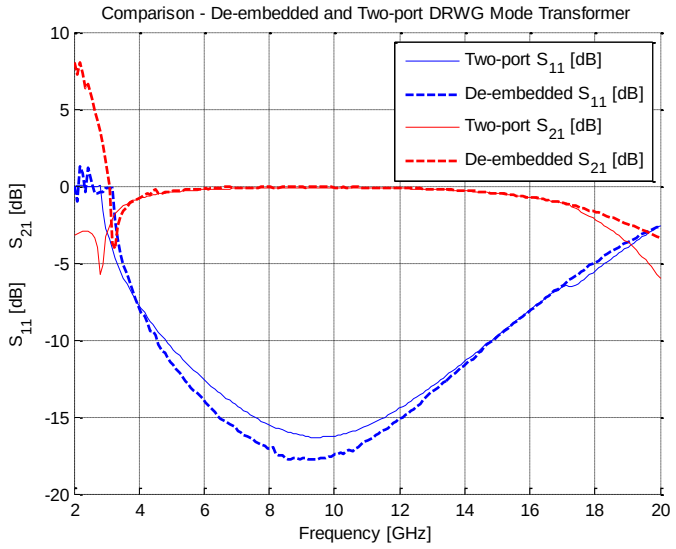

Figure 6.7. Comparison of the de-embedded and the two-port measurement reflection and transmission responses of the shortened coaxial to double ridged waveguide mode transformer.

The three offset short measurements were processed with the MATLAB algorithm. The comparison of the de-embedded and two-port characterisation results is shown in figure 6.7.

Reducing the distance between the mode transformer pin and the backshort has shifted the quarter wavelength transformer to occur at 20 GHz, which is outside the possible workable bandwidth of the model. Furthermore reducing the length of the waveguide has shifted the three-quarter wavelength transformer to also present outside the possible workable bandwidth. This results in a very good correlation between the two-port FEKO characterisation and the three offset short characterisation of the mode transformer.

The three offset short measurements were then processed in the C++ application. The comparison of the FEKO, MATLAB and C++ responses is shown in figure 6.8.

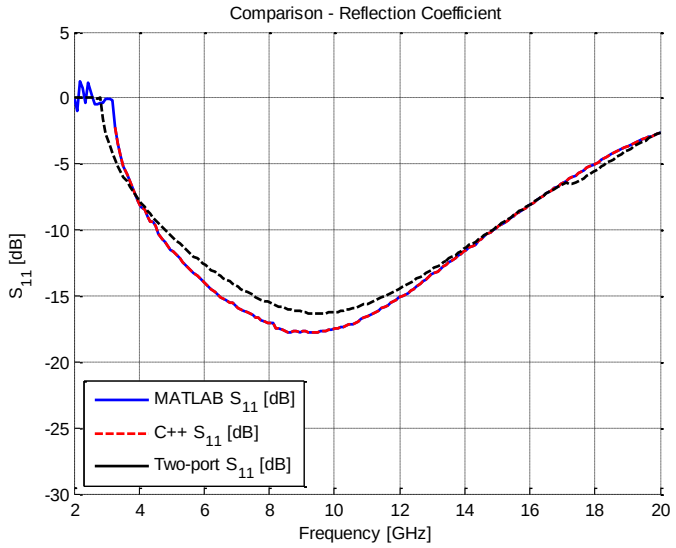

Figure 6.8. A comparison of the reflection coefficient of the mode transformer obtained from FEKO, the MATLAB algorithm and the C++ application.

The de-embedded reflection coefficients from both the MATLAB algorithm and the C++ application are effectively identical, and both are in very good agreement with the reflection coefficient obtained from the two-port FEKO characterisation.

6.4 SUMMARY

A coaxial to double ridged waveguide mode transformer was designed and characterised using the three offset short de-embedding method.

The design was based on the Sivers Lab PM 7325X mode transformer. Thereafter a parametric study of the ridge dimensions was performed to result in a coaxial to double ridged waveguide mode transformer with a centre frequency of 10 GHz. The structure was modelled in FEKO and the three offset short de-embedding method was performed to characterise the structure. As a reference of the performance of the structure a fourth measurement was made by terminating the mode transformer in a matched load.

The de-embedded results were in good agreement with the results obtained from the matched load measurement with the exception of the singularities that occurred at 15.5 GHz, 18 GHz and 19 GHz. These were found to be as a result of the length between the mode transformer pin and the backshort of the structure. Furthermore the length between the mode transformer pin and the first offset short termination was influencing the occurrence of one of the singularities. This was addressed by reducing the length between the pin and the backshort as well as reducing the length of the waveguide section of the structure and reducing the offsets of the short terminations. The de-embedding of the shortened structure was in very good agreement with the matched load measurement of the same structure and presented with none of the singularities observed for the initial structure.

The three offset short de-embedding method presents an effective way of characterising a coaxial to double ridged waveguide mode transformer. The strengths of this de-embedding method are in that it only requires the use of Delay and Short electrical standards, which are well characterised and can easily be obtained for double ridged waveguide structures. It does however present inherent limitations related to the internal lengths of the structure. However, by altering these lengths the effects of the singularities can be shifted outside the desired frequency range.

CHAPTER 7

DISCUSSION AND CONCLUSION

7.1 General Conclusions

The characterisation of the properties of a DUT often requires the DUT to be placed in an embedding network to match the terminations of the DUT to the terminations of the measurement device. However, the presence of the embedding structure obscures the properties of the DUT as it imparts its own properties on the measurement. Consequently, the objective of this work was the development of an analysis mechanism for the purpose of characterising the embedding network, also referred to as error network characterisation.

A method to extract the properties of the DUT from the properties of the measurement was needed. To this end a large variety of de-embedding methods were evaluated to identify a de-embedding method, or a combination of de-embedding methods, which could be used for the development of a network characterisation mechanism.

The evaluated de-embedding methods were organised into two distinct classes, namely the analytically based class of de-embedding method and the numerically based class of de-embedding methods. It was found that the latter class is better suited to performing the characterisation of a network that is implemented in a CAD environment. Alternatively, the latter class of de-embedding methods can be used for purposes of network optimisation. In both cases the physical dimensions of the DUT need to be well defined.

The analytically based class of de-embedding methods was identified as being a more robust approach to de-embedding as the precise physical dimensions of the error network do not need to be known for characterisation to be performed and can thus be applied to the characterisation of an arbitrary TEM network or network with only a single propagating mode . The de-embedding is performed by taking measurements of the network with the DUT replaced with known electrical standards and then solving the

closed form equations which describe the reflection and transmission properties of the network.

The analysis mechanism was based on the analytically based class of de-embedding methods. Of the de-embedding methods discussed in that class the three offset short de-embedding method was identified as being the best suited for the purposes of network characterisation as it requires the use of only Delay and Short electrical standards. Both of these electrical standards are well described for networks used in Microwave Engineering.

The three offset short de-embedding method was at first implemented in a MATLAB algorithm and applied to perform the characterisation of a lumped element lowpass filter test network. The properties of the test network were also evaluated using a ladder analysis method and the two sets of properties were compared. The de-embedding method was found to perform satisfactorily, albeit for the occurrence of a singularity at the cutoff frequency of the lowpass filter. Based on these results the MATLAB algorithm was then implemented into a C++ based application.

The three offset short de-embedding method was further tested by applying it to characterise three different mode transformer networks used as feeds for, amongst others, antennas. The three feed networks used were the parallel line feed, the coaxial to rectangular waveguide mode transformer and the coaxial to double ridged waveguide mode transformer. In all three cases the analysis mechanism performed the characterisation satisfactorily. However, the occurrence of singularities was observed in the properties obtained from the de-embedding method.

The singularities, which occurred in all the results obtained from the analysis mechanism, were identified as an inherent limitation of the three offset short de-embedding method. At certain frequencies the choice of the Delay electrical standard length behaves as a quarter wavelength transformer. The effects of the quarter wavelength transformer caused the Short termination to be measured at the reference plane as an Open termination. As the de-

embedding method algorithm is defined to make use of Short electrical standards as terminations this transformation presented as a singularity in the transmission properties of the network.

The occurrence of the singularities is directly related to the choice of offset length. One way to remove the singularity from presenting in the desired frequency range is by careful choice of the offset lengths, thus allowing the singularity to occur outside the frequency range.

Another way is by replacing the offset length related to the quarter wavelength transformer with a fourth, different offset length and performing the characterisation again. This will cause the singularity at a different frequency. By superimposing the two sets of de-embedded properties the singularities are removed.

Alternatively, in the case of the coaxial to double ridged waveguide, the reference planes and backshort of the model can be shifted to a position closer to the mode transformer causing the singularities to be shifted to occur outside the desired frequency range. However, for cases where changing the dimensions of the structure might not be possible, careful choice of offset lengths is necessary. By choosing the first offset short to be located a quarter wavelength away from the reference plane, at the frequency of the singularity, and the subsequent offset shorts to be located a further half a wavelength away from the previous short location, allows the occurrence of the singularity to be eliminated at that frequency. Thereafter, superimposing the sets of de-embedded properties removes the singularity form the S-parameters.

7.2 Application of the Analysis Mechanism and Future Work

The developed analysis mechanism can be applied to the characterisation of either a TEM network or a network supporting only a single propagating mode, of which only basic structural properties need to be known. These include the type of structure, e.g. rectangular

waveguide which is needed to determine the propagation constant of the structure at a specific mode, and the physical lengths of the three offsets. The effects of higher order modes were not investigated in this work and thus this remains a topic for further study.

The mechanism is not only limited to the characterisation of antenna feed networks but can also be applied to the characterisation of subsections of a DUT. A network is defined by the location of the reference planes. As the locations of the reference planes can be defined arbitrarily, as long as they remain constant throughout the de-embedding procedure, they can thus be defined inside the network. Using a three stub microstrip filter as an example, the reference planes of this network are generally defined to contain the three stubs in between the device terminals. However, by defining the reference planes to contain only two of the network stubs it is possible for the properties of only those two stubs to be characterised, making it possible to internally analyse a network.

A method of characterising the properties of an error network has been developed. If the error network, which has to be characterised by means of the developed analysis mechanism, is connected to a DUT, as is shown in figure 1.1.(a), the properties of the network can be measured or calculated and from the network properties the properties of the DUT can be isolated. For instance, a study of the properties of an antenna, where the antenna is the DUT, can be performed irrespective of the properties of the mode transformer used to feed the antenna as the properties of the mode transformer can be eliminated from the measurement or calculation of the network. Thus, a study of a double or quad ridged horn entails choosing an arbitrary mode transformer, characterising it, and then extracting the properties of the horn from the properties of the horn and mode transformer network measurement or calculation, as long as the mode transformer guide and the horn guide are the same.

REFERENCES

[1] R. F. Bauer and P. Penfield Jr., "De-Embedding and Unterminating," *IEEE Trans. Microw. Theory Tech.*, vol. 22, no. 3, pp. 282- 288, Mar. 1974.

[2] R. Lane, "De-embedding device scattering parameters," *Microw. J.*, pp. 149-156, Aug. 1984.

[3] N. R. Franzen and R. A. Speciale, "A New Procedure for System Calibration and Error Removal in Automated S-Parameter Measurements," *5th Euro. Microw. Conf.*, pp. 69-73, 1-4 Sep. 1975.

[4] G. F. Engen and C. A. Hoer, "Thru-Reflect-Line: An Improved Technique for Calibrating the Dual Six-Port Automatic Network Analyzer," *IEEE Trans. Microw. Theory Tech.*, vol. 27, no. 12, pp. 987- 993, Dec. 1979.

[5] D. F. Williams and T. H. Miers, "De-embedding coplanar probes with planar distributed standards," *IEEE Trans. Microw. Theory Tech.*, vol. 36, no. 12, pp. 1876-1880, Dec. 1988.

[6] M. B. Steer, S. B. Goldberg, G. Rinne, P. D. Franzon, I. Turlik, J. S. Kasten, "Introducing the through-line deembedding procedure," *IEEE MTT-S Int. Microw. Symp. Dig.*, vol. 3, pp. 1455-1458, 1-5 Jun. 1992.

[7] H. J. Eul and B. Schiek, "Thru-Match-Reflect: One Result of a Rigorous Theory for De-Embedding and Network Analyzer Calibration," *18th Euro. Microw. Conf.*, pp. 909-914, 12-15 Sep. 1988.

[8] J. A. Reynoso-Hernandez and E. Inzunza-Gonzalez, "A Straightforward De-Embedding Method for Devices Embedded in Test Fixtures," *57th ARFTG Conf. Digest-Spring*, vol. 39, pp. 1-5, May 2001.

[9] J. C. Rautio, "A de-embedding algorithm for electromagnetics," *Int. J. Microw. Millimeter-Wave Comput.-Aided Eng.*, vol. 1, no. 3, pp. 282–287, Jul. 1991.

[10] J. E. Zuniga-Juarez, J. A. Reynoso-Hernandez, and J. R. Loo-Yau, "Two-tier L-L de-embedding method for S-parameters measurements of devices mounted in test fixture," *73rd ARFTG Microw. Measure. Conf.*, pp. 1-5, 12 Jun. 2009.

[11] H. Heuermann and B. Schiek, "Line network network (LNN): an alternative in-fixture calibration procedure," *IEEE Trans. Microw. Theory Tech.*, vol. 45, no. 3, pp. 408-413, Mar. 1997.

[12] E. S. Daniel, N. E. Harff, V. Sokolov, S. M. Schreiber, and B. K. Gilbert, "Network analyzer measurement de-embedding utilizing a distributed transmission matrix bisection of a single THRU structure," *63rd ARFTG Conf. Digest-Spring*, pp. 61- 68, 11 Jun. 2004.

[13] E. F. da Silva and M. K. McPhun, "Calibration of microwave network analyser for computer-corrected S parameter measurements," *Electron. Lett.*, vol. 9, no. 6, pp. 126-128, 22 Mar. 1973.

[14] E. F. da Silva and M. K. McPhun, "Calibration of an automatic network analyser using transmission lines of unknown characteristic impedance, loss and dispersion," *Radio Electron. Eng.*, vol. 48, no. 5, pp. 227-234, May 1978.

[15] B. Kolundzija, B. Janic, and M. Rakic, "Novel technique for deembedding S-parameters in electromagnetic modeling of arbitrary circuits," *IEEE Ant. Prop. Soc. Int. Symp.*, vol. 3, pp. 2784-2787, 20-25 Jun. 2004.

[16] R. L. Vaitkus, "Wide-band de-embedding with a short, an open, and a through line," *Proc. IEEE*, vol. 74, no. 1, pp. 71-74, Jan. 1986.

[17] A. Ferrero and U. Pisani, "Two-port network analyzer calibration using an unknown `thru'," *IEEE Microw. Guided Wave Lett.*, vol. 2, no. 12, pp. 505-507, Dec. 1992.

[18] S. R. Pennock, C. M. D. Rycroft, P. R. Shepherd, and T. Rozzi, "Transition Characterisation for De-Embedding Purposes," *17th Euro. Microw. Conf.*, pp. 355-360, 7-11 Sep. 1987.

[19] H. Liang, J. Laskar, M. Hyslop, and R. Panicker, "A Novel De-embedding Technique for Millimeter-wave Package Characterization," *54th ARFTG Conf. Digest-Spring*, vol. 36, pp. 1-8, Dec. 2000.

[20] X. Hongya and E. Kasper, "A de-embedding procedure for one-port active mm-wave devices," *Top. Meet. Silicon Monolithic Integ. Circ. in RF Syst. (SiRF)*, pp. 37-40, 11-13 Jan. 2010.

[21] M. C. A. M. Koolen, J. A. M. Geelen, and M. P. J. G. Versleijen, "An improved de-embedding technique for on-wafer high-frequency characterization," *Proc. Bipolar Circ. Techno. Meet.*, pp. 188-191, 9-10 Sep. 1991.

[22] C. Ming-Hsiang, H. Guo-Wei, W. Yueh-Hua and W. Lin-Kun, "A scalable noise de-embedding technique for on-wafer microwave device characterization," *IEEE Microw. Wireless Comp. Lett.*, vol. 15, no. 10, pp. 649- 651, Oct. 2005.

[23] C. Wan, B. Nauwelears, W. De Raedt, and M. Van Rossum, ""1 Thru+2.5 Reflects": A new technique for de-embedding MIC/MMIC device measurements in fixed-length fixtures," *26th Euro. Microw. Conf.*, vol. 1, pp. 174-177, 6-13 Sep. 1996.

[24] C. Hsiu-Ying, H. Jiun-Kai, K. Chin-Wei, S. Liu, and W. Chung-Yu, ”A Novel Transmission-Line Deembedding Technique for RF Device Characterization,” *IEEE Trans. Electron. Devices*, vol. 56, no. 12, pp. 3160-3167, Dec. 2009.

[25] N. Li, K. Matsushita, N. Takayama, S. Ito, K. Okada, and A. Matsuzawa, “Evaluation of a multi-line de-embedding technique up to 110 GHz for millimeter-wave CMOS circuit design,” *IEICE Trans. Fundamentals*, vol. E93-A, no. 2, pp. 431-439, Feb. 2010.

[26] Y. Tretiakov, K. Vaed, W. Woods, S. Venkatadri, and T. Zwick, “A new on-wafer de-embedding technique for on-chip RF transmission line interconnect characterization,” *63rd ARFTG Conf. Digest-Spring*, pp. 69- 72, 11 Jun. 2004.

[27] L. See Chuan, L. Fujiang, and X. Yong Ping, “An improved NL-L transmission line de-embedding technique for mm-wave applications,” *IEEE Int. Symp. RF Integr. Tech.*, pp. 133-136, 9 Jan. 2009-11 Dec. 2009.

[28] J. M. Song, F. Ling, W. Blood, E. Demircan, K. Sriram, G. Flynn, K. H. To, R. Tsai, Q. Li, and T. Myers, “De-embedding techniques for embedded microstrips,” *Microw. Opt. Tech. Lett.*, vol. 42, no. 1, pp. 50-54, 2004.

[29] T. Sekiguchi, S. Amakawa, N. Ishihara, and K. Masu, “On the validity of bisection-based thru-only de-embedding,” *IEEE Int. Conf. Microelectron. Test Struct. (ICMTS)*, pp. 66-71, 22-25 Mar. 2010.

[30] W. K. Gwarek, “Analysis of arbitrarily shaped two-dimensional microwave circuits by finite difference time domain method,” *IEEE Trans. Microw. Theory Tech.*, vol. 36, pp. 738-744, Apr. 1988.

[31] D. M. Sheen, S. M. Ali, M. D. Abonzahra, and J. A. Kong, “Application of the three-dimensional finite-difference time-domain method to the analysis of planar microstrip circuits,” *IEEE Trans. Ant. Prop.*, vol. 38, pp. 849-857, Jul. 1990.

[32] G. V. Eleftheriades and R. Mosig, “On the network characterization of planar passive circuits using the method of moments,” *IEEE Trans. Microw. Theory Tech.*, vol. 44, pp. 438–445, Mar. 1996.

[33] L. Zhu and K. Wu, “Characterization of unbounded multiport microstrip passive circuits using an explicit network-based method of moments,” *IEEE Trans. Microw. Theory Tech.*, vol. 45, no. 12, pp. 2114-2124, 1997.

[34] L. Zhu and K. Wu, “Unified equivalent-circuit model of planar discontinuities suitable for field theory-based CAD and optimization of M(H)MIC’s,” *IEEE Trans. Microw. Theory Tech.*, vol. 47, pp. 1589–1602, Sep. 1999.

[35] M. Farina and T. Rozzi, "A short-open deembedding technique for method-of-moments-based electromagnetic analyses," *IEEE Trans. Microw. Theory Tech.*, vol. 49, no. 4, pp. 624-628, Apr. 2001.

[36] R. Sorrentino, "Numerical methods for passive components," *IEEE MTT-S Int. Microw. Sym. Dig.*,vol. 2, pp. 619-622, 25-27 May 1988.

[37] I. Munteanu and I. Hanninen, "Recent advances in CST STUDIO SUITE for antenna simulation," *6th Euro. Conf. Ant. Prop. (EUCAP)*, pp. 1301-1305, 26-30 Mar. 2012.

[38] R. S. Chen, D. X. Wang, and E. K. N.Yung, "Application of the short-open calibration technique to vector finite element method for analysis of microwave circuits," *Int. J. Numer. Model.*, vol. 16, pp. 367–385, 2003.

[39] A. S. Adalev, N. V. Korovkin, and M. Hayakawa, "De-embedding microwave fixtures with the genetic algorithm," *IEEE 6th Int. Symp. Electromag. Compat. Electromag. Ecol.*, pp. 190- 194, 21-24 Jun. 2005.

[40] A. J. Lozano-Guerrero, J. Monzó-Cabrera, F. J. Clemente-Fernández, J. L. Pedreño-Molina, and A. Díaz-Morcillo, "Coaxial to waveguide transitions and device under test characterization by means of inverse techniques," *Microw. Opt. Tech. Lett.*, vol. 52, pp. 1294–1297., 2010.

[41] Agilent Technologies, "Network Analysis Applying the 8510 TRL Calibration for Non-Coaxial Measurements," *Net. Anal. Appl. 8510 TRL Calib. Non-Coax. Measure.*, 8510, Product Note 8510- 8A, 2001.

[42] D. Rytting, "ARFTG 50 year network analyzer history," *IEEE MTT-S Int. Microw. Symp. Dig.*, pp. 11-18, 15-20 Jun. 2008.

[43] C. G. Montgomery, R. H. Dicke, and E. M. Purcell, *Princ. Microw. Circ.*, 1st ed., New York: McGraw-Hill, 1948, p. 90.

[44] S. J. Mason, "Feedback Theory-Further Properties of Signal Flow Graphs," *Proc. IRE*, vol. 44, no. 7, pp. 920-926, Jul. 1956.

[45] *HP Application Note 95-1*, "S-parameter techniques for faster, more accurate network design" Hewlett-Packard, 1997.

[46] J. Frei, X.-D. Cai, and S. Muller, "Multiport S-parameter and T- parameter conversion with symmetry extension," *IEEE Trans. Microw. Theory Tech.*, vol. 56, no. 11, pp. 2493–2504, Nov. 2008.

[47] R. C. Dorf and R. H. Bishop, "Signal-Flow Graph Models," in *Modern Control Systems*, 11th ed. New Jersey, Prentice Hall, 2007, ch. 2, sec. 2.7, pp. 76-82.

[48] G. J. Scalzi, A. J. Slobodnik Jr., and G. A. Roberts, "Network analyzer calibration using offset shorts," *IEEE Trans. Microw. Theory Tech.*, vol. 36, no. 6, pp. 1097-1100, Jun. 1988.

[49] J. A. G. Malherbe, "Hybrid elliptic TEM horn with symmetric main beam," *15th Int. Symp. Ant. Techn. Appl. Electromag. (ANTEM)*, pp. 1-4, 25-28 Jun. 2012.

[50] W. J. R. Hoefer and M. N. Burton, "Closed-Form Expressions for the Parameters of Finned and Ridged Waveguides," *IEEE Trans. Microw. Theory Tech.*, vol. 30, no. 12, pp. 2190-2194, Dec. 1982.

[51] *FEKO Examples Guide*, Suite 6.1, Example 20., EMSS (Pty) Ltd., Stellenbosch, South Africa, 2011.

[52] S. Hopfer, "The Design of Ridged Waveguides," *IRE Trans. Microw. Theory Tech.*, vol. 3, no. 5, pp. 20-29, Oct. 1955.

[53] S. B. Cohn, "Properties of Ridge Wave Guide," *Proc. IRE*, vol. 35, no. 8, pp. 783- 788, Aug. 1947.